

International Journal of Modern Physics D
 © World Scientific Publishing Company

Is excess smoothing of Planck CMB anisotropy data partially responsible for evidence for dark energy dynamics in other $w(z)$ CDM parametrizations?

Chan-Gyung Park

*Division of Science Education and Institute of Fusion Science, Jeonbuk National University,
 Jeonju 54896, Republic of Korea
 park.chan.gyung@gmail.com*

Bharat Ratra

*Department of Physics, Kansas State University, 116 Cardwell Hall, Manhattan, KS 66506,
 USA
 ratra@ksu.edu*

Received Day Month Year

Revised Day Month Year

We study spatially-flat dynamical dark energy parametrizations, $w(z)$ CDM, with redshift-dependent dark energy equation of state parameter $w(z)$ expressed using three different quadratic and other polynomial forms (as functions of $1 - a$, where a is the scale factor), without and with a varying cosmic microwave background (CMB) lensing consistency parameter A_L . We use Planck CMB anisotropy data (P18 and lensing) and a large, mutually-consistent non-CMB data compilation that includes Pantheon+ type Ia supernova, baryon acoustic oscillation (BAO), Hubble parameter ($H(z)$), and growth factor ($f\sigma_8$) measurements, but not recent DESI BAO data. The six $w(z)$ CDM ($+A_L$) parametrizations show higher consistency between the CMB and non-CMB data constraints compared to the Λ CDM ($+A_L$) and w_0w_a CDM ($+A_L$) cases. Constraints from the most-restrictive P18+lensing+non-CMB data compilation on the six $w(z)$ CDM ($+A_L$) parametrizations indicate that dark energy dynamics is favored over a cosmological constant by $\gtrsim 2\sigma$ when $A_L = 1$, but only by $\gtrsim 1\sigma$ when A_L is allowed to vary (and $A_L > 1$ at $\sim 2\sigma$ significance). Non-CMB data dominate the P18+lensing+non-CMB compilation at low z and favor quintessence-like dark energy. At high z P18+lensing data dominate, favoring phantom-like dark energy with significance from 1.5σ to 2.9σ when $A_L = 1$, and from 1.1σ to 1.8σ when A_L varies. These results suggest that the observed excess weak lensing smoothing of some of the Planck CMB anisotropy multipoles is partially responsible for the $A_L = 1$ cases $\gtrsim 2\sigma$ evidence for dark energy dynamics over a cosmological constant.

Keywords: dark energy; cosmological parameters; cosmic background radiation.

PACS numbers: 98.80.-k

1. Introduction

In the standard spatially-flat Λ CDM cosmological model,¹ dark energy in the form of a cosmological constant Λ dominates the current cosmological energy budget and is

responsible for the observed, low-redshift, accelerated cosmological expansion, with cold dark matter (CDM) being the next largest contributor to the current energy budget. This flat Λ CDM model agrees with many of the observational constraints, but there are some clouds, for recent reviews see Refs. 2–5.

A recent example is the DESI Collaboration result⁶ determined from observational data analyzed in the spatially-flat w_0w_a CDM parametrization in which dynamical dark energy is taken to be a fluid with a parameterized equation of state parameter (the ratio of the fluid pressure to the fluid energy density) $w(a) = w_0 + w_a(1 - a) = w_0 + w_az/(1 + z) = w(z)$, a function of redshift z or cosmological scale factor a .^{7,8} The analysis of new DESI baryon acoustic oscillation (BAO) measurements in combination with cosmic microwave background (CMB) data and Type Ia supernova (SNIa) observations, in particular the DESI+CMB+PantheonPlus data compilation, see Ref. 6 for a detailed description, indicates that these data favor a region in parameter space that is $\gtrsim 2\sigma$ away from the flat Λ CDM model point at $w_0 = -1$ and $w_a = 0$,⁶ thus indicating $\gtrsim 2\sigma$ support for dynamical dark energy over a cosmological constant. For discussions of the DESI result, see Refs. 9–57 and references therein.

In the w_0w_a CDM parametrization the $\gtrsim 2\sigma$ support for dynamical dark energy over a cosmological constant does not require including DESI BAO measurements or SNIa data in the analysis.¹⁹ A large compilation of independent, mutually-consistent, non-CMB measurements⁵⁸ used jointly with Planck CMB anisotropy data⁵⁹ provide slightly more restrictive constraints and support for dark energy dynamics¹⁹ than found from the DESI+CM+PantheonPlus compilation.⁶ And there have been earlier suggestions that dynamical dark energy is mildly favored over a cosmological constant, see Refs. 60–74 and references therein.

While the $\gtrsim 2\sigma$ support for dark energy dynamics in the w_0w_a CDM parametrization does not require using DESI BAO data or SNIa data in the analysis,¹⁹ part of this support seems to be related to the observed excess weak lensing smoothing of some Planck CMB anisotropy multipoles (relative to what is predicted in the Planck best-fit cosmological model),^{59,75} as follows, Ref. 50. Including the lensing consistency parameter A_L ⁷⁵ in the analysis, as a new free parameter to be determined from the dataset being analyzed, allows for a consistency check on the excess weak lensing smoothing. If the dataset under analysis gives a value of A_L that is consistent with unity then there is no excess smoothing. In the standard flat Λ CDM model, Planck CMB anisotropy data give $A_L > 1$ at $\sim 2\sigma$, indicating that there is excess smoothing.^{59,76} Including a varying A_L in an analysis of Planck CMB data and non-CMB data in the w_0w_a CDM+ A_L parametrization:⁵⁰ makes the Planck CMB data constraints and the non-CMB data constraints more consistent; again results in an $A_L > 1$ at $\sim 2\sigma$; and, reduces the support for dark energy dynamics over a cosmological constant to $\gtrsim 1\sigma$, compared to the $A_L = 1$ case support of $\gtrsim 2\sigma$, thus suggesting that the observed excess smoothing of some Planck CMB anisotropy multipoles contributes to the $\gtrsim 2\sigma$ support for dark energy dynamics in the $A_L = 1$ w_0w_a CDM parametrization.

In this study we extend earlier work^{19,50} by exploring three new spatially-flat $w(z)$ CDM ($+A_L$) dynamical dark energy parametrizations with $w(z)$ expressed in quadratic and other polynomial forms as a function of $1 - a$. Utilizing the largest independent and mutually-consistent compilation of non-CMB data to date⁵⁸ together with Planck CMB data, we study these parametrizations to address the important question of whether dark energy exhibits dynamics beyond the cosmological constant. Through a combined analysis of the CMB (P18 and lensing) and non-CMB data compilation, we observationally constrain these dynamical dark energy parametrizations (without and with a varying CMB lensing consistency parameter A_L) and quantitatively investigate how well they fit the observations and how consistent the CMB and non-CMB data constraints are with each other in a given parametrization. We find from results of the analyses of the six $w(z)$ CDM ($+A_L$) parametrizations (including $A_L = 1$ and varying A_L cases) that there is better consistency between the CMB and non-CMB data constraints than in the simpler Λ CDM ($+A_L$) parametrizations with constant dark energy equation of state and in the w_0w_a CDM ($+A_L$) parametrizations. In all six cases, the best-fit dark energy is dynamical and has quintessence-like behavior at low z and phantom-like behavior at high z . In the $A_L = 1$ cases dark energy dynamics is favored over a cosmological constant at $\gtrsim 2\sigma$, however in the varying A_L cases this support reduces to $\gtrsim 1\sigma$ (with $A_L > 1$ at $\sim 2\sigma$). This again suggests that the observed excess smoothing of some Planck CMB anisotropy multipoles contributes to the $\gtrsim 2\sigma$ support for dark energy dynamics in the three new $A_L = 1$ $w(z)$ CDM parametrizations we study here, consistent with the w_0w_a CDM($+A_L$) findings of Ref. 50.

In Sec. 2 we provide brief details of the data sets we use to constrain cosmological parameters in, and test the performance of, the flat $w(z)$ CDM parametrizations. In Sec. 3 we briefly summarize the main features of the three flat w_0w_2 CDM, w_0w_p CDM, and $w_0w_1w_2$ CDM parametrizations we study and the analysis techniques we use. Our results are presented and discussed in Sec. 4, and we conclude in Sec. 5.

2. Data

In this paper CMB and non-CMB data sets are used to constrain the parameters of dynamical dark energy parameterizations. The data sets we use for this purpose are described in detail in Sec. II of Ref. 58 and outlined in what follows. We account for all known data covariances.

For the CMB data, we use the Planck 2018 TT,TE,EE+lowE (P18) CMB temperature and polarization power spectra alone as well as jointly with the Planck lensing potential (lensing) power spectrum.^{59,77}

The non-CMB data set we use is the non-CMB (new) data compilation of Ref. 58, which is comprised of

- 16 BAO data points, spanning $0.122 \leq z \leq 2.334$, listed in Table I of Ref. 58. We do not use DESI 2024 BAO data.⁶

- A 1590 SNIa data point subset of the Pantheon+ compilation,⁷⁸ retaining only SNIa with $z > 0.01$ to mitigate peculiar velocity correction effects. These data span $0.01016 \leq z \leq 2.26137$,
- 32 Hubble parameter $[H(z)]$ measurements, spanning $0.070 \leq z \leq 1.965$, listed in Table 1 of Ref. 79 and in Table II of Ref. 58.
- An additional nine (non-BAO) growth rate ($f\sigma_8$) data points, spanning $0.013 \leq z \leq 1.36$, listed in Table III of Ref. 58.

We use five individual and combined data sets to constrain the flat $w(z)$ CDM models with three different dark energy equation of state parametrizations: P18 data, P18+lensing data, non-CMB data, P18+non-CMB data, and P18+lensing+non-CMB data.

3. Methods

Here we summarize the method we applied in this study. Additional details about the methodology we use are described in Sec. III of Ref. 58.

To determine quantitatively how restrictively these observational data constrain cosmological model parameters, we make use of the `CAMB/COSMOMC` program (October 2018 version).^{80–82} `CAMB` computes the evolution of spatial inhomogeneities and makes theoretical predictions which depend on the cosmological parameters of the dynamical dark energy parameterizations we study here. `COSMOMC` uses the Markov chain Monte Carlo (MCMC) method to compare these theoretical model predictions to observational data, to determine cosmological parameter likelihoods. The MCMC chains are assumed to have converged when the Gelman and Rubin R statistic (provided by `COSMOMC`) satisfies $R - 1 < 0.01$. For each model and data set, we use the converged MCMC chains, with the `GetDist` code,⁸³ to compute the average values, confidence intervals, and likelihood distributions of model parameters.

To establish a baseline for comparison, we also study the spatially-flat Λ CDM model. The six primary cosmological parameters for this model are conventionally chosen to be the current value of the physical baryonic matter density parameter $\Omega_b h^2$, the current value of the physical cold dark matter density parameter $\Omega_c h^2$, the angular size of the sound horizon at recombination $100\theta_{\text{MC}}$, the optical depth to reionization τ , the scalar-type primordial perturbation power spectral index n_s , and the power spectrum amplitude $\ln(10^{10} A_s)$, where h is the Hubble constant in units of $100 \text{ km s}^{-1} \text{ Mpc}^{-1}$. We assume flat priors for these parameters, non-zero over: $0.005 \leq \Omega_b h^2 \leq 0.1$, $0.001 \leq \Omega_c h^2 \leq 0.99$, $0.5 \leq 100\theta_{\text{MC}} \leq 10$, $0.01 \leq \tau \leq 0.8$, $0.8 \leq n_s \leq 1.2$, and $1.61 \leq \ln(10^{10} A_s) \leq 3.91$. In the flat Λ CDM+ A_L model (and the $w(z)$ CDM+ A_L parametrizations), for the lensing consistency parameter A_L we adopt a flat prior non-zero over $0 \leq A_L \leq 10$.

In the $w_0 w_a$ CDM parameterization dynamical dark energy is assumed to be a fluid with an evolving equation of state parameter (fluid pressure to energy density ratio) $w(a) = w_0 + w_a(1 - a)$ as a function of scale factor a or equivalently $w(z) = w_0 + w_a z/(1 + z)$ as a function of redshift z .^{7,8} Since this two parameter

dynamical dark energy parameterization explores a specific dark energy equation of state parameter region, we also study an extended three parameter $w_0w_1w_2$ CDM parametrization that includes the quadratic term,

$$w(a) = w_0 + w_1(1 - a) + w_2(1 - a)^2. \quad (1)$$

When $w_2 = 0$ and with $w_1 = w_a$, this reduces to the w_0w_a CDM parameterization. (Higher order terms are also possible,⁸⁴ but current data do not as effectively constrain dynamical dark energy parameterizations with four or more free parameters.) We first explore the two parameter w_0w_2 CDM case with $w_1 = 0$, and then the more general case where w_0 , w_1 , and w_2 all vary.

We also consider an extension of the quadratic ($w_1 = 0$) case to an arbitrary order p form, with the three parameter w_0w_p CDM parameterization,

$$w(a) = w_0 + w_p(1 - a)^p, \quad (2)$$

where the order p is an additional dark energy parameter, in addition to w_0 and w_p .

In all cases we consider here and in Refs. 19,50, at low redshift these $w(z)$ CDM parameterizations behave like an Λ CDM parameterization with $w_0 = w(z = 0)$, while at high redshift they also behave like an Λ CDM parameterization but now with $w(z \rightarrow \infty) = w_0 + w_a$ (for w_0w_a CDM), $= w_0 + w_2$ (for w_0w_2 CDM), $= w_0 + w_p$ (for w_0w_p CDM), and $= w_0 + w_1 + w_2$ (for $w_0w_1w_2$ CDM). Compared to Λ CDM, these two- and three-parameter $w(z)$ CDM parameterizations have more flexibility in fitting data, allowing $w(z = 0)$ to better fit low-redshift non-CMB data while $w(z \rightarrow \infty)$ can now better accommodate high-redshift CMB data. To allow for dynamical dark energy parameterizations whose equation of state parameter crosses $w = -1$, the CAMB/COSMOMC option of the parametrized post-Friedmann dark energy model⁸⁵ is used.

For the dynamical dark energy equation of state parameters in the w_0w_a CDM model parameterization we adopt flat priors non-zero over $-3.0 \leq w_0 \leq 0.2$ and $-3 < w_a < 2$. For the w_0w_p CDM parameterization, we apply an additional flat prior for the p parameter non-zero over $0 \leq p \leq 4$ while the flat prior for w_p is non-zero over $-3 \leq w_p \leq 2$. In the $w_0w_1w_2$ CDM parameterization we adopt an additional flat prior non-zero over $-3 \leq w_2 \leq 2$ with w_1 having the same prior as w_a .

When we estimate parameters using non-CMB data, we fix the values of τ and n_s to those obtained from P18 data (since these parameters cannot be determined solely from non-CMB data) and constrain the other cosmological parameters.

Additionally, we also present constraints on three derived parameters: the Hubble constant H_0 , the current value of the non-relativistic matter density parameter Ω_m , and the amplitude of matter fluctuations σ_8 , that are determined from those on the primary parameters of the cosmological model. We also record the values of the sum of dark energy equation of state parameters to which $w(z)$ approaches at high z , in the different dynamical dark energy parameterizations we study: $w_0 + w_a$,

6 *Park & Ratra*

$w_1 + w_2 + w_3$, $w_0 + w_2$, and $w_0 + w_p$. These are determined from the primary parameters of the corresponding dynamical dark energy parametrization.

All the $w(z)$ CDM parametrizations we study here, as well as the Λ CDM model, have flat spatial hypersurfaces and a tilted scalar-type primordial scalar-type energy density perturbation power spectrum

$$P_\delta(k) = A_s \left(\frac{k}{k_0} \right)^{n_s}, \quad (3)$$

where k is the wavenumber and n_s and A_s are the spectral index and the amplitude and the power spectrum at pivot scale $k_0 = 0.05 \text{ Mpc}^{-1}$. This power spectrum is sourced by zero-point quantum fluctuations during an early epoch of power-law inflation in a spatially-flat inflation model with a scalar field inflaton potential energy density that is an exponential function of the inflaton.^{86–88}

Table 1. Consistency check parameter $\log_{10} \mathcal{I}$ and tension parameters σ and p (%) for P18 vs. non-CMB datasets and P18+lensing vs. non-CMB datasets in the flat w_0w_2 CDM, w_0w_2 CDM+ A_L , w_0w_pp CDM, w_0w_pp CDM+ A_L , $w_0w_1w_2$ CDM, and $w_0w_1w_2$ CDM+ A_L models.

		Flat w_0w_2 CDM model		Flat w_0w_2 CDM+ A_L model	
Data		P18 vs non-CMB	P18+lensing vs non-CMB	P18 vs non-CMB	P18+lensing vs non-CMB
$\log_{10} \mathcal{I}$		-0.605	-0.496	0.202	0.186
σ		2.538	2.462	1.833	1.851
p (%)		1.114	1.381	6.685	6.412
		Flat w_0w_pp CDM model		Flat w_0w_pp CDM+ A_L model	
Data		P18 vs non-CMB	P18+lensing vs non-CMB	P18 vs non-CMB	P18+lensing vs non-CMB
$\log_{10} \mathcal{I}$		-0.411	-0.308	0.344	0.358
σ		2.461	2.315	1.678	1.842
p (%)		1.386	2.064	9.341	6.545
		Flat $w_0w_1w_2$ CDM model		Flat $w_0w_1w_2$ CDM+ A_L model	
Data		P18 vs non-CMB	P18+lensing vs non-CMB	P18 vs non-CMB	P18+lensing vs non-CMB
$\log_{10} \mathcal{I}$		-0.609	-0.649	0.431	0.231
σ		2.615	2.589	1.872	1.901
p (%)		0.894	0.964	6.124	5.727

To quantify how relatively well each model fits the dataset under consideration, we use differences in the Akaike information criterion (ΔAIC) and deviance information criterion (ΔDIC) between the information criterion (IC) values for the $w(z)$ CDM parametrization under study and the Λ CDM model. See Sec. III of Ref. 58 for a fuller discussion. According to the Jeffreys' scale we use, when $-2 \leq \Delta\text{IC} < 0$ there is *weak* evidence in favor of the model under study, when $-6 \leq \Delta\text{IC} < -2$ there is *positive* evidence, when $-10 \leq \Delta\text{IC} < -6$ there is *strong* evidence, and when $\Delta\text{IC} < -10$ there is *very strong* evidence in favor of the model under study

Is excess smoothing of Planck data partially responsible for DE dynamics in $w(z)$ CDM? 7

relative to the tilted flat Λ CDM model. This scale also holds when ΔIC is positive, but then the flat Λ CDM model is favored over the $w(z)$ CDM parametrization under study.

To quantitatively compare how consistent the cosmological parameter constraints (for the same parametrization) derived from two different data sets are, we use two estimators. The first is the DIC based $\log_{10} \mathcal{I}$, see Ref. 89 and Sec. III of Ref. 58. When the two data sets are consistent $\log_{10} \mathcal{I} > 0$ while $\log_{10} \mathcal{I} < 0$ means that the two data sets are inconsistent. According to the Jeffreys' scale we use, the degree of consistency or inconsistency between two data sets is *substantial* if $|\log_{10} \mathcal{I}| > 0.5$, *strong* if $|\log_{10} \mathcal{I}| > 1$, and *decisive* if $|\log_{10} \mathcal{I}| > 2$.⁸⁹ The second estimator is the tension probability p and the related, Gaussian approximation, "sigma value" σ , see Refs. 90–92 and Sec. III of Ref. 58. $p = 0.05$ and $p = 0.003$ correspond to 2σ and 3σ Gaussian standard deviation, respectively.

4. Results and Discussion

Table 1 lists the values of the two statistical estimators, $\log_{10} \mathcal{I}$ and p values, that measure the consistency between cosmological parameter constraints from P18 and non-CMB data and from P18+lensing and non-CMB data, for the three pairs of $w(z)$ CDM and $w(z)$ CDM+ A_L parametrizations we study in this paper. Compared to the corresponding values of the two statistical estimators in the w_0w_a CDM and w_0w_a CDM+ A_L cases,^{19,50} the values here for all six parametrizations we study indicate better consistency between the pairs of dataset constraints. Patterns similar to those seen in Refs. 19, 50 for the w_0w_a CDM (+ A_L) parametrizations are also found here. Allowing A_L to vary increases the consistency between the pairs of dataset constraints, but even for the $A_L = 1$ cases the pairs of dataset constraints agree to better than 3σ . As these dataset constraints are consistent, in the following we mostly focus on results from the largest dataset, the P18+lensing+non-CMB one.

Tables 2 and 3 summarize the parameter constraints for the w_0w_2 CDM (+ A_L) parametrizations. The likelihood distributions of the cosmological parameters are shown in Figures 1–4, with just the w_0 , w_2 , and $w_0 + w_2$ panels shown in Figures 5 and 6. Tables 4 and 5 summarize the parameter constraints for the w_0w_p CDM (+ A_L) parametrizations. The likelihood distributions of the cosmological parameters are shown in Figure 7–10, with just the w_0 , w_p , p , and $w_0 + w_p$ panels shown in Figures 11 and 12. Tables 6 and 7 summarize the parameter constraints for the $w_0w_1w_2$ CDM (+ A_L) parametrizations. The likelihood distributions of the cosmological parameters are shown in Figure 13–16, with just the w_0 , w_1 , w_2 , and $w_0 + w_1 + w_2$ panels shown in Figures 17 and 18. Tables 2–7 also list the $\Delta\chi_{\min}^2$, ΔAIC , and ΔDIC values.

As in the w_0w_a CDM (+ A_L) cases^{19,50} the constraints on the $w(z)$ parameters, as well as on the derived parameters H_0 , Ω_m , and σ_8 , from P18 and from P18+lensing data are less restrictive than those from non-CMB data.

We first compare the cosmological parameter values determined from

Table 2. Mean and 68% (or 95%) confidence limits of flat w_0w_2 CDM model parameters from non-CMB, P18, P18+lensing, P18+non-CMB, and P18+lensing+non-CMB data. H_0 has units of $\text{km s}^{-1} \text{Mpc}^{-1}$. We also list the values of χ^2_{\min} , DIC, and AIC and the differences with respect to the values in the flat Λ CDM model for the same dataset, denoted by $\Delta\chi^2_{\min}$, Δ DIC, and Δ AIC, respectively.

Parameter	Non-CMB	P18	P18+lensing	P18+non-CMB	P18+lensing+non-CMB
$\Omega_b h^2$	$0.0311^{+0.0039}_{-0.0045}$	0.02240 ± 0.00015	0.02243 ± 0.00015	0.02243 ± 0.00014	0.02244 ± 0.00014
$\Omega_c h^2$	$0.1011^{+0.0065}_{-0.012}$	0.1199 ± 0.0014	0.1193 ± 0.0012	0.1192 ± 0.0011	0.11917 ± 0.00099
$100\theta_{\text{MC}}$	$1.0234^{+0.0092}_{-0.011}$	1.04094 ± 0.00031	1.04100 ± 0.00030	1.04098 ± 0.00030	1.04098 ± 0.00030
τ	0.0540	0.0540 ± 0.0079	0.0520 ± 0.0075	0.0523 ± 0.0078	0.0527 ± 0.0074
n_s	0.9655	0.9655 ± 0.0043	0.9668 ± 0.0042	0.9668 ± 0.0040	0.9668 ± 0.0038
$\ln(10^{10}A_s)$	$3.54 \pm 0.27 (> 3.04)$	3.043 ± 0.016	3.037 ± 0.015	3.038 ± 0.016	3.039 ± 0.014
w_0	-0.864 ± 0.040	$-1.46^{+0.21}_{-0.44}$	$-1.44^{+0.21}_{-0.45}$	-0.898 ± 0.041	-0.898 ± 0.040
w_2	$-0.01^{+0.63}_{-0.25}$	$-1.1 \pm 1.3 (< 1.24)$	$-1.0 \pm 1.3 (< 1.34)$	$-1.12^{+0.51}_{-0.42}$	$-1.12^{+0.50}_{-0.40}$
$w_0 + w_2$	$-0.88^{+0.62}_{-0.23}$	$-2.56^{+0.90}_{-1.5}$	$-2.5^{+1.0}_{-1.6}$	$-2.02^{+0.48}_{-0.39}$	$-2.02^{+0.47}_{-0.37}$
H_0	$69.8^{+2.2}_{-2.5}$	$85 \pm 10 (> 66.0)$	$85 \pm 10 (> 66.7)$	67.90 ± 0.64	67.94 ± 0.64
Ω_m	$0.2724^{+0.0095}_{-0.017}$	$0.207^{+0.014}_{-0.065}$	$0.208^{+0.015}_{-0.066}$	0.3087 ± 0.0063	0.3083 ± 0.0063
σ_8	$0.819^{+0.031}_{-0.027}$	$0.961^{+0.11}_{-0.045}$	$0.951^{+0.11}_{-0.045}$	0.812 ± 0.011	0.8125 ± 0.0091
χ^2_{\min}	1457.50	2761.24	2770.45	4233.13	4241.78
$\Delta\chi^2_{\min}$	-12.43	-4.56	-4.26	-7.11	-7.48
DIC	1470.99	2815.85	2824.55	4289.62	4297.81
Δ DIC	-7.12	-2.08	-1.90	-2.71	-3.39
AIC	1469.50	2819.24	2828.45	4291.13	4299.78
Δ AIC	-8.43	-0.56	-0.26	-3.11	-3.48

P18+lensing+non-CMB data for the eight-parameter w_0w_2 CDM and the nine-parameter w_0w_2 CDM+ A_L parametrizations that are listed in the last columns of Tables 2 and 3. Differences in the values of the six primary parameters common to the flat Λ CDM model are smaller than 1σ : $\Omega_b h^2$ (-0.54σ), $\Omega_c h^2$ ($+0.82\sigma$), $100\theta_{\text{MC}}$ (-0.37σ), τ ($+0.42\sigma$), n_s (-0.67σ), and $\ln(10^{10}A_s)$ ($+0.64\sigma$). For the two equation of state parameters, for the w_0w_2 CDM parametrization we find $w_0 = -0.898 \pm 0.040$ and $w_2 = -1.12^{+0.50}_{-0.40}$ while for the w_0w_2 CDM+ A_L parametrization we have $w_0 = -0.908 \pm 0.040$ and $w_2 = -0.78^{+0.48}_{-0.39}$, with the difference between these pair of values being $+0.18\sigma$ and -0.54σ . For the high- z asymptotic value of $w(z)$, $w_0 + w_2$, we find for the w_0w_2 CDM parametrization $w_0 + w_2 = -2.02^{+0.47}_{-0.37}$ while for the w_0w_2 CDM+ A_L parametrization $w_0 + w_2 = -1.69^{+0.45}_{-0.36}$, with a -0.56σ difference between the two results. For the derived parameters H_0 , Ω_m , and σ_8 , the differences are $+0.01\sigma$, $+0.28\sigma$, and $+1.03\sigma$, respectively.

We now compare the cosmological parameter values determined from P18+lensing+non-CMB data for the nine-parameter w_0w_p pCDM and the ten-parameter w_0w_p pCDM+ A_L parametrizations that are listed in the last columns of Tables 4 and 5. Differences in the values of the six primary parameters common to the flat Λ CDM model are smaller than 1σ : $\Omega_b h^2$ (-0.49σ), $\Omega_c h^2$ ($+0.80\sigma$), $100\theta_{\text{MC}}$ (-0.28σ), τ ($+0.43\sigma$), n_s (-0.60σ), and $\ln(10^{10}A_s)$ ($+0.61\sigma$). For the three equation of state parameters, for the w_0w_p pCDM parametrization we find

Is excess smoothing of Planck data partially responsible for DE dynamics in $w(z)$ CDM? 9

Table 3. Mean and 68% (or 95%) confidence limits of flat w_0w_2 CDM+ A_L model parameters from non-CMB, P18, P18+lensing, P18+non-CMB, and P18+lensing+non-CMB data. H_0 has units of $\text{km s}^{-1} \text{Mpc}^{-1}$. We also list the values of χ^2_{\min} , DIC, and AIC and the differences with respect to the values in the flat Λ CDM model for the same dataset, denoted by $\Delta\chi^2_{\min}$, Δ DIC, and Δ AIC, respectively.

Parameter	Non-CMB	P18	P18+lensing	P18+non-CMB	P18+lensing+non-CMB
$\Omega_b h^2$	$0.0311^{+0.0039}_{-0.0045}$	0.02258 ± 0.00017	0.02250 ± 0.00017	0.02263 ± 0.00016	0.02255 ± 0.00015
$\Omega_c h^2$	$0.1011^{+0.0065}_{-0.012}$	0.1182 ± 0.0015	0.1184 ± 0.0015	0.1177 ± 0.0012	0.1179 ± 0.0012
$100\theta_{\text{MC}}$	$1.0234^{+0.0092}_{-0.011}$	1.04114 ± 0.00033	1.04108 ± 0.00032	1.04119 ± 0.00032	1.04114 ± 0.00031
τ	0.0540	0.0494 ± 0.0087	$0.0495^{+0.0085}_{-0.0073}$	$0.0481^{+0.0089}_{-0.0074}$	0.0480 ± 0.0083
n_s	0.9654	0.9706 ± 0.0049	0.9690 ± 0.0048	0.9718 ± 0.0044	0.9706 ± 0.0042
$\ln(10^{10} A_s)$	$3.54 \pm 0.27 (> 3.04)$	3.030 ± 0.018	$3.030^{+0.018}_{-0.016}$	$3.026^{+0.018}_{-0.015}$	3.025 ± 0.017
A_L	...	$1.164^{+0.064}_{-0.087}$	$1.046^{+0.040}_{-0.055}$	1.186 ± 0.066	1.072 ± 0.038
w_0	-0.864 ± 0.040	$-1.15^{+0.35}_{-0.65}$	$-1.28^{+0.27}_{-0.58}$	-0.909 ± 0.040	-0.908 ± 0.040
w_2	$-0.01^{+0.63}_{-0.25}$	$-1.0 \pm 1.3 (< 1.24)$	$-0.9 \pm 1.3 (< 1.35)$	$-0.73^{+0.48}_{-0.38}$	$-0.78^{+0.48}_{-0.39}$
$w_0 + w_2$	$-0.88^{+0.62}_{-0.23}$	$-2.1^{+1.4}_{-1.2}$	-2.2 ± 1.2	$-1.64^{+0.45}_{-0.35}$	$-1.69^{+0.45}_{-0.36}$
H_0	$69.8^{+2.2}_{-2.5}$	$77^{+20}_{-8} (> 53.4)$	$80 \pm 13 (> 57.6)$	67.96 ± 0.63	67.93 ± 0.63
Ω_m	$0.2724^{+0.0095}_{-0.017}$	$0.268^{+0.038}_{-0.013}$	$0.240^{+0.022}_{-0.099}$	0.3052 ± 0.0062	0.3058 ± 0.0062
σ_8	$0.819^{+0.031}_{-0.027}$	$0.868^{+0.16}_{-0.085}$	$0.901^{+0.15}_{-0.066}$	0.795 ± 0.012	0.797 ± 0.012
χ^2_{\min}	1457.50	2755.88	2770.27	4222.49	4237.66
$\Delta\chi^2_{\min}$	-12.43	-9.92	-4.44	-17.75	-11.60
DIC	1470.99	2813.08	2825.76	4283.13	4295.89
Δ DIC	-7.12	-4.85	-0.69	-9.20	-5.31
AIC	1469.50	2815.88	2830.27	4282.49	4297.66
Δ AIC	-8.43	-3.92	+1.56	-11.75	-5.60

$w_0 = -0.916^{+0.031}_{-0.045}$, $w_p = -1.73^{+0.48}_{-1.2}$, and $p = 2.86^{+1.1}_{-0.26} (> 1.31)$ while for the w_0w_p CDM+ A_L parametrization we have $w_0 = -0.917^{+0.032}_{-0.042}$, $w_p = -1.34^{+1.1}_{-0.69}$, and $p = 2.8 \pm 0.9 (> 1.01)$, with the difference between these triplets of values being $+0.02\sigma$, -0.46σ , and $+0.06\sigma$. For the high- z asymptotic value of $w(z)$, $w_0 + w_p$, we find for the w_0w_p CDM parametrization $w_0 + w_p = -2.65^{+0.54}_{-1.1}$ while for the w_0w_p CDM+ A_L parametrization $w_0 + w_p = -2.26^{+1.2}_{-0.63}$, with a -0.47σ difference between the two results. For the derived parameters H_0 , Ω_m , and σ_8 , the differences are $+0.01\sigma$, $+0.26\sigma$, and $+0.96\sigma$, respectively.

We finally compare the cosmological parameter values determined from P18+lensing+non-CMB data for the nine-parameter $w_0w_1w_2$ CDM and the ten-parameter $w_0w_1w_2$ CDM+ A_L parametrizations that are listed in the last columns of Tables 6 and 7. Differences in the values of the six primary parameters common to the flat Λ CDM model are smaller than 1σ : $\Omega_b h^2$ (-0.49σ), $\Omega_c h^2$ ($+0.85\sigma$), $100\theta_{\text{MC}}$ (-0.33σ), τ ($+0.42\sigma$), n_s (-0.64σ), and $\ln(10^{10} A_s)$ ($+0.64\sigma$). For the three equation of state parameters, for the $w_0w_1w_2$ CDM parametrization we find $w_0 = -0.929^{+0.077}_{-0.095}$, $w_1 = 0.27^{+0.87}_{-0.45}$, and $w_2 = -1.5 \pm 1.1 (< 0.709)$ while for the $w_0w_1w_2$ CDM+ A_L parametrization we have $w_0 = -0.943^{+0.083}_{-0.095}$, $w_1 = 0.31^{+0.94}_{-0.54}$, and $w_2 = -1.2 \pm 1.2 (< 1.08)$, with the difference between these triplets of values being $+0.11\sigma$, -0.04σ , and -0.18σ . For the high- z asymptotic value of $w(z)$, $w_0 + w_1 + w_2$,

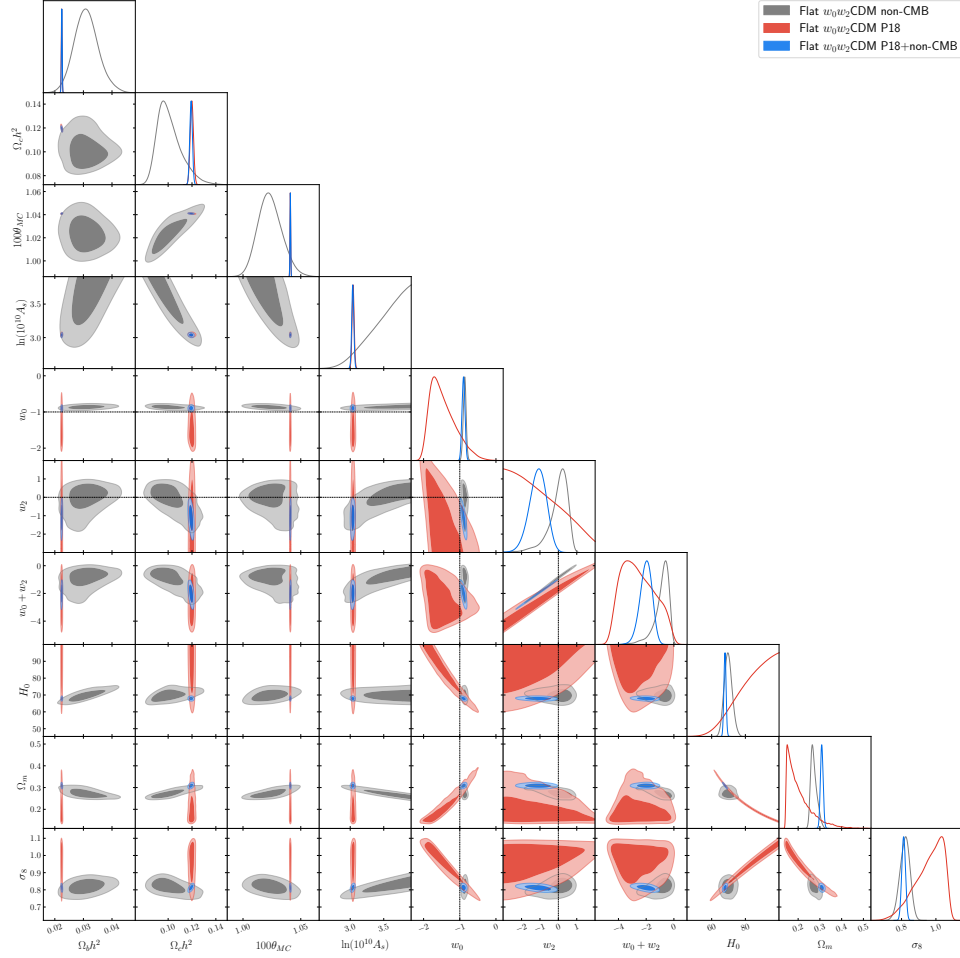


Fig. 1. One-dimensional likelihoods and 1σ and 2σ likelihood confidence contours of flat w_0w_2 CDM model parameters favored by non-CMB, P18, and P18+non-CMB datasets. We do not show τ and n_s , which are fixed in the non-CMB data analysis.

we find for the $w_0w_1w_2$ CDM parametrization $w_0 + w_1 + w_2 = -2.15^{+0.40}_{-0.71}$ while for the $w_0w_1w_2$ CDM+ A_L parametrization $w_0 + w_1 + w_2 = -1.88^{+0.50}_{-0.79}$, with a -0.30σ difference between the two results. For the derived parameters H_0 , Ω_m , and σ_8 , the differences are -0.04σ , $+0.34\sigma$, and $+0.99\sigma$, respectively.

To assess how relatively-well these spatially-flat dynamical dark energy parametrizations do in fitting the P18+lensing+non-CMB dataset, we compare their DIC values, more precisely their Δ DIC values relative to the DIC value of the standard flat Λ CDM model. These Δ DIC values are listed in Tables 2–7 here, with the flat w_0w_a CDM (+ A_L) values listed in tables 1 and 2 of Ref. 50, the flat XCDM+ A_L parametrization value listed in table XI of Ref. 58 (in the flat XCDM

Is excess smoothing of Planck data partially responsible for DE dynamics in $w(z)$ CDM? 11

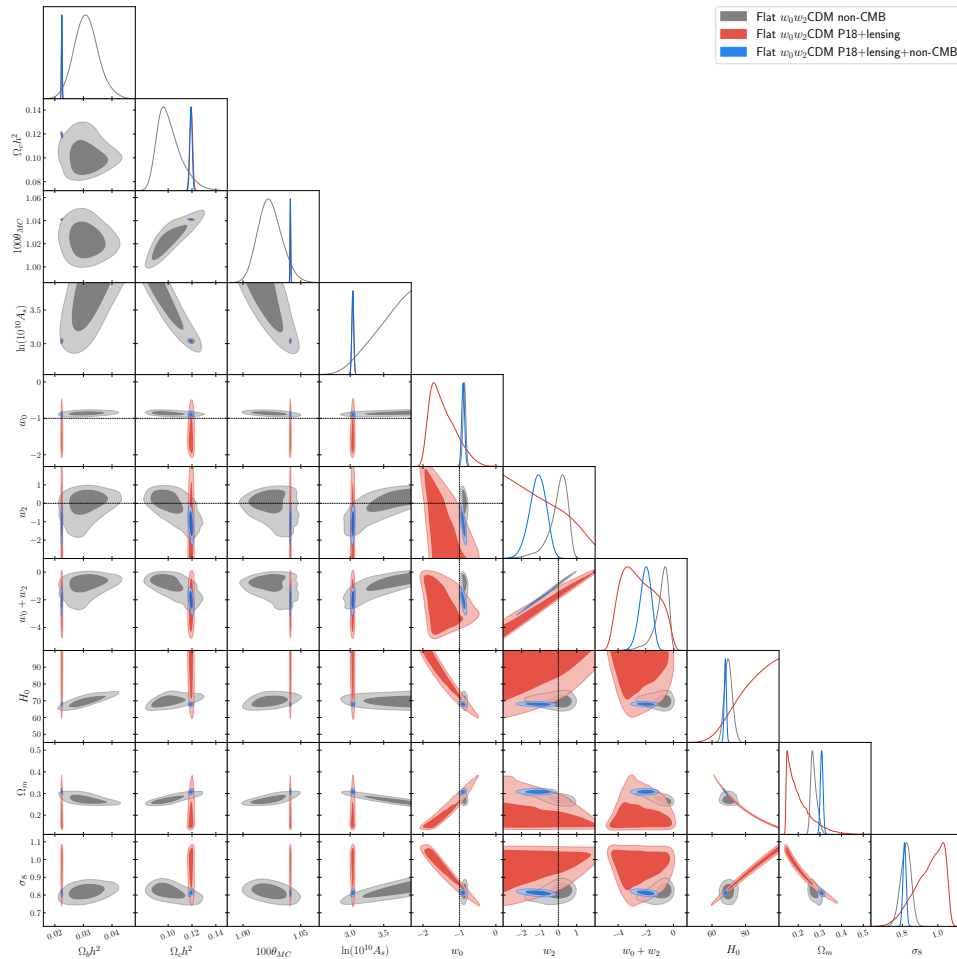


Fig. 2. One-dimensional likelihoods and 1σ and 2σ likelihood confidence contours of flat w_0w_2 CDM model parameters favored by non-CMB, P18+lensing, P18+lensing+non-CMB datasets. We do not show τ and n_s , which are fixed in the non-CMB data analysis.

parametrization with $A_L = 1$ the P18+lensing and the non-CMB cosmological constraints are inconsistent at 3.6σ , ruling the parametrization out at this significance, see Ref. 58), and the flat Λ CDM+ A_L value listed in table VII of Ref. 58. There is *positive* evidence in favor of all models and parametrizations relative to the flat Λ CDM model, with the w_0w_{pp} CDM+ A_L parametrization with $\Delta\text{DIC} = -5.60$ favored the most and the w_0w_a CDM parametrization with $\Delta\text{DIC} = -2.45$ favored the least over the flat Λ CDM model.

We now investigate whether the largest data compilation we study, the P18+lensing+non-CMB dataset, provides model-independent cosmological parameter constraints by comparing these constraints in several dark energy models and

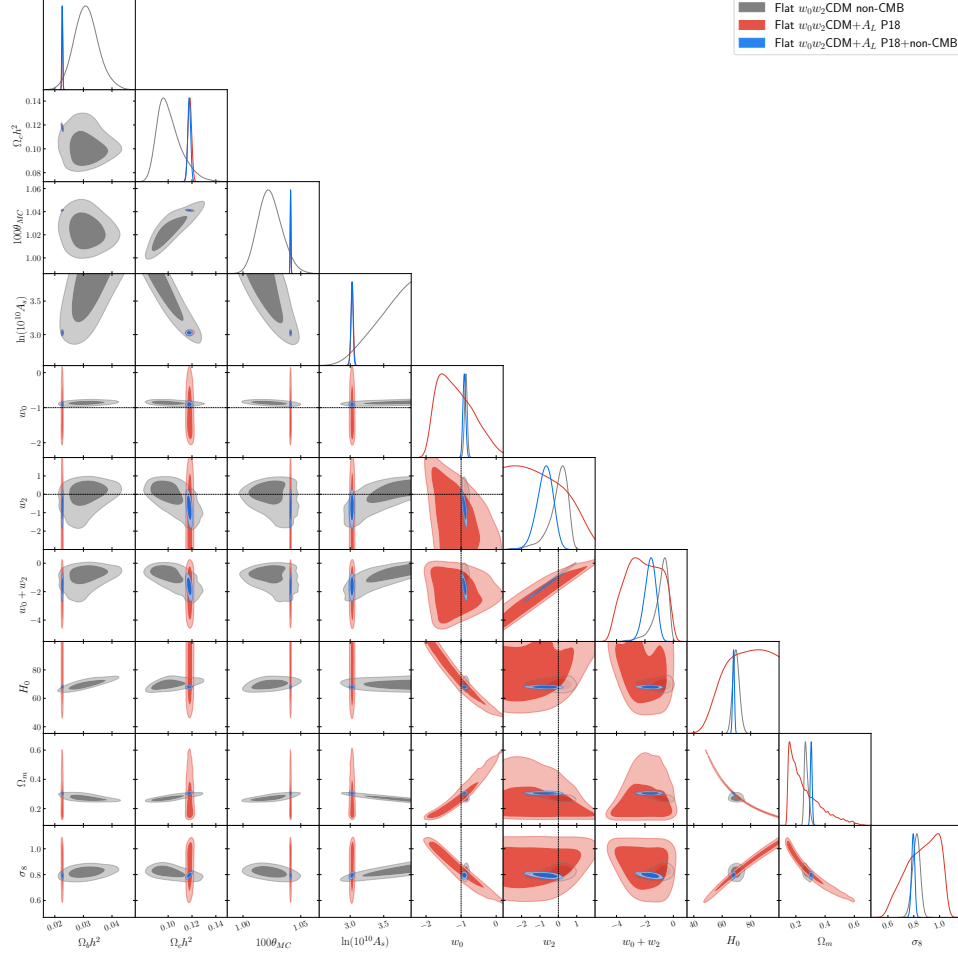


Fig. 3. One-dimensional likelihoods and 1σ and 2σ likelihood confidence contours of flat $w_0w_2\text{CDM}+A_L$ model parameters favored by non-CMB, P18, and P18+non-CMB datasets. We do not show τ and n_s , which are fixed in the non-CMB data analysis.

parametrizations. The P18+lensing+non-CMB data parameter constraints for the flat $\Lambda\text{CDM} (+A_L)$ models are in tables IV and VII of Ref. 58, while those for the flat XCDM ($+A_L$) parametrization are in table XI there. In this analysis we do not consider the flat XCDM parametrization with $A_L = 1$ since P18+lensing constraints and non-CMB constraints are more than 3σ inconsistent in this case.⁵⁸ P18+lensing+non-CMB data parameter constraints for the flat $w_0w_a\text{CDM} (+A_L)$ parametrizations are in table 1 and 2 of Ref. 50, while those of the flat $w_0w_2\text{CDM} (+A_L)$, $w_0w_p\text{CDM} (+A_L)$, and $w_0w_1w_2\text{CDM} (+A_L)$ parametrizations are in Tables 2–7.

We first consider the $A_L = 1$ flat dark energy models and parametrizations and

Is excess smoothing of Planck data partially responsible for DE dynamics in $w(z)$ CDM? 13

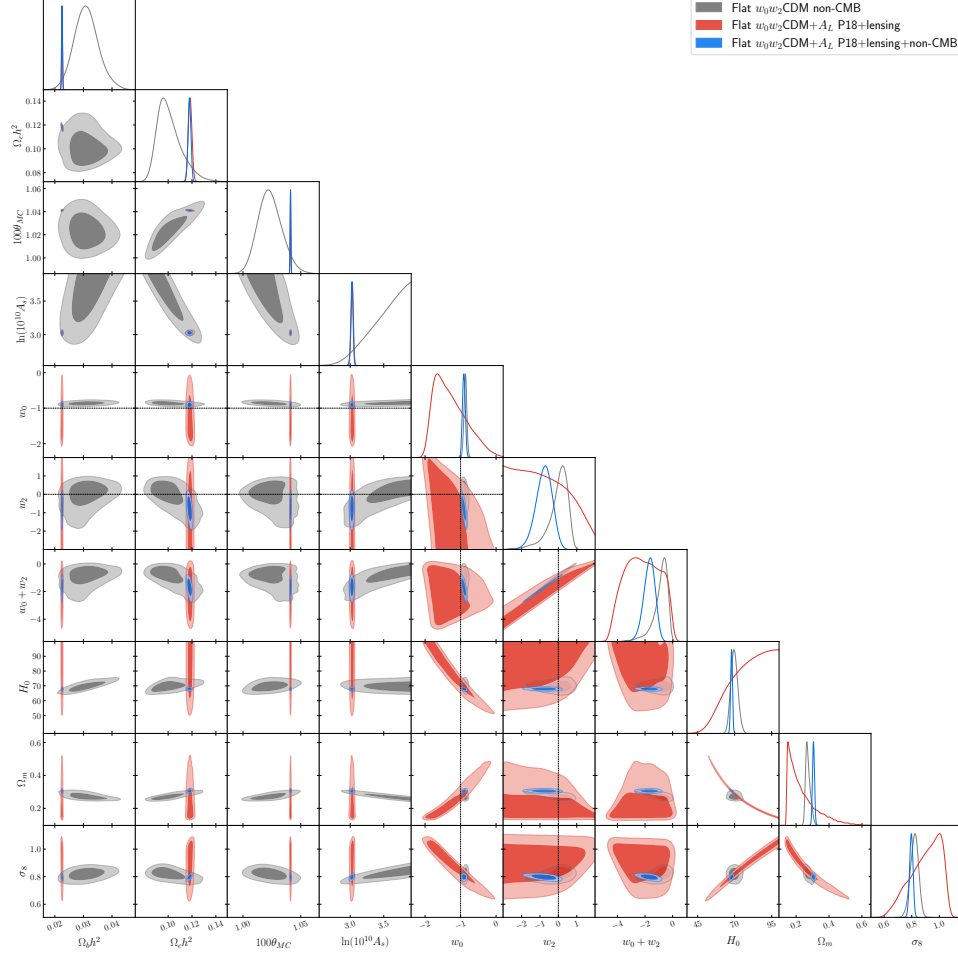


Fig. 4. One-dimensional likelihoods and 1σ and 2σ likelihood confidence contours of flat w_0w_2 CDM+ A_L model parameters favored by non-CMB, P18+lensing, P18+lensing+non-CMB datasets. We do not show τ and n_s , which are fixed in the non-CMB data analysis.

first compute the largest model-to-model differences for the six common model parameters. For $\Omega_b h^2$ the largest value is 0.02249 ± 0.00013 in the Λ CDM model and the smallest is 0.02244 ± 0.00014 in the w_0w_a CDM and w_0w_2 CDM parametrizations, resulting in a difference of 0.26σ . For $\Omega_c h^2$ the smallest value is 0.11849 ± 0.00084 in the Λ CDM model and the largest is 0.11917 ± 0.00099 in the w_0w_2 CDM parametrization, resulting in a difference of 0.52σ . For $100\theta_{MC}$ the Λ CDM model $100\theta_{MC} = 1.04109 \pm 0.00028$ is the largest and the w_0w_2 CDM parametrization $100\theta_{MC} = 1.04098 \pm 0.00030$ is the smallest, giving a difference of 0.27σ . For τ and n_s the largest deviation is 0.41σ and 0.32σ , respectively, between the largest Λ CDM model values ($\tau = 0.0569 \pm 0.0071$ and $n_s = 0.9685 \pm 0.0036$) and the smallest

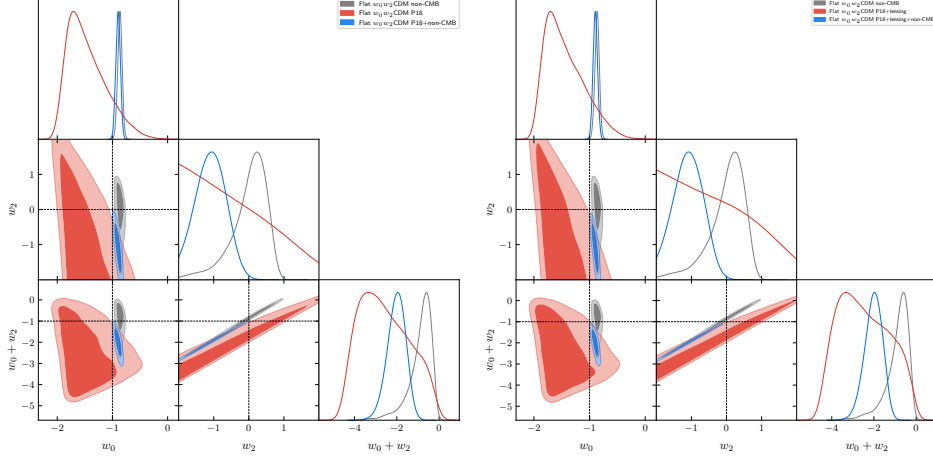


Fig. 5. One-dimensional likelihoods and 1σ and 2σ likelihood confidence contours of w_0 , w_2 , and $w_0 + w_2$ parameters in the flat w_0w_2 CDM parametrization favored by (left) non-CMB, P18, and P18+non-CMB datasets, and (right) non-CMB, P18+lensing, and P18+lensing+non-CMB datasets.

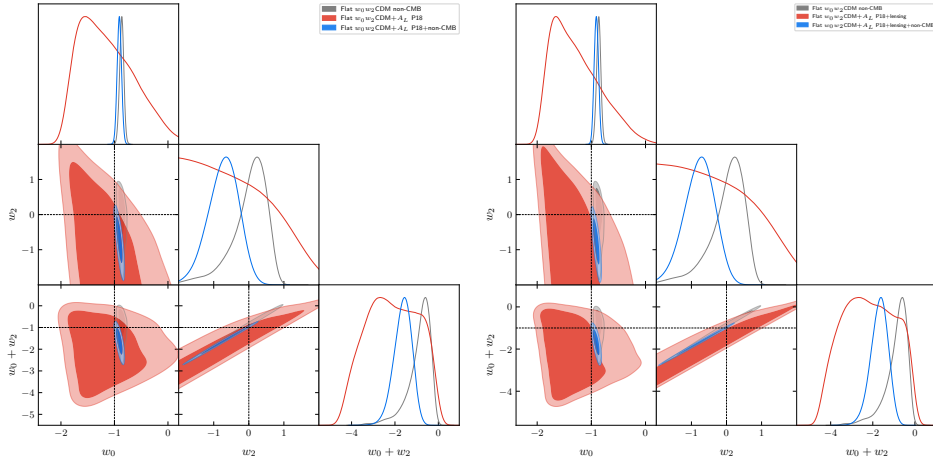


Fig. 6. One-dimensional likelihoods and 1σ and 2σ likelihood confidence contours of w_0 , w_2 , and $w_0 + w_2$ parameters in the flat w_0w_2 CDM+ A_L parametrization favored by (left) non-CMB, P18, and P18+non-CMB datasets, and (right) non-CMB, P18+lensing, and P18+lensing+non-CMB datasets.

w_0w_2 CDM parametrization values ($\tau = 0.0527 \pm 0.0074$ and $n_s = 0.9668 \pm 0.0038$). For $\ln(10^{10} A_s)$ the Λ CDM model largest value ($\ln(10^{10} A_s) = 3.046 \pm 0.014$) and the w_0w_2 CDM, w_0w_p CDM, and $w_0w_1w_2$ CDM parametrizations smallest value ($\ln(10^{10} A_s) = 3.039 \pm 0.014$) differ at 0.35σ . Thus for $A_L = 1$ the six common model parameters agree between the various dark energy models and parametriza-

Is excess smoothing of Planck data partially responsible for DE dynamics in $w(z)$ CDM? 15

Table 4. Mean and 68% (or 95%) confidence limits of flat w_0w_p CDM model parameters from non-CMB, P18, P18+lensing, P18+non-CMB, and P18+lensing+non-CMB data. H_0 has units of $\text{km s}^{-1} \text{Mpc}^{-1}$. We also list the values of χ^2_{\min} , DIC, and AIC and the differences with respect to the values in the flat Λ CDM model for the same dataset, denoted by $\Delta\chi^2_{\min}$, Δ DIC, and Δ AIC, respectively.

Parameter	Non-CMB	P18	P18+lensing	P18+non-CMB	P18+lensing+non-CMB
$\Omega_b h^2$	0.0308 ± 0.0044	0.02239 ± 0.00015	0.02243 ± 0.00015	0.02245 ± 0.00014	0.02245 ± 0.00014
$\Omega_c h^2$	$0.1014^{+0.0073}_{-0.012}$	0.1199 ± 0.0014	0.1193 ± 0.0012	0.1191 ± 0.0011	0.11904 ± 0.00098
$100\theta_{\text{MC}}$	$1.0228^{+0.0097}_{-0.011}$	1.04094 ± 0.00031	1.04099 ± 0.00031	1.04100 ± 0.00030	1.04101 ± 0.00030
τ	0.0540	0.0540 ± 0.0079	0.0522 ± 0.0075	0.0527 ± 0.0077	0.0530 ± 0.0073
n_s	0.9655	0.9655 ± 0.0044	0.9667 ± 0.0041	0.9672 ± 0.0039	0.9671 ± 0.0038
$\ln(10^{10} A_s)$	$3.52 \pm 0.26 (> 3.06)$	3.044 ± 0.016	3.038 ± 0.015	3.038 ± 0.016	3.039 ± 0.014
w_0	$-0.865^{+0.048}_{-0.041}$	$-1.40^{+0.29}_{-0.55}$	$-1.39^{+0.26}_{-0.53}$	$-0.914^{+0.031}_{-0.046}$	$-0.916^{+0.031}_{-0.045}$
w_p	$-0.25^{+0.95}_{-0.23}$	$-1.0 \pm 1.3 (< 1.36)$	$-1.0 \pm 1.3 (< 1.35)$	$-1.70^{+0.52}_{-1.2}$	$-1.73^{+0.48}_{-1.2}$
p	$2.5 \pm 1.1 (> 0.454)$	$1.93^{+0.87}_{-1.7} (> 0.257)$	$2.0 \pm 1.1 (> 0.276)$	$2.8 \pm 0.8 (> 1.20)$	$2.86^{+1.1}_{-0.26} (> 1.31)$
$w_0 + w_p$	$-1.11^{+0.96}_{-0.19}$	$-2.4^{+1.1}_{-1.3}$	$-2.4^{+1.1}_{-1.3}$	$-2.61^{+0.54}_{-1.2}$	$-2.65^{+0.54}_{-1.1}$
H_0	69.7 ± 2.4	$86 \pm 10 (> 66.8)$	$85 \pm 10 (> 66.8)$	67.89 ± 0.63	67.92 ± 0.64
Ω_m	$0.273^{+0.011}_{-0.017}$	$0.205^{+0.013}_{-0.062}$	$0.205^{+0.014}_{-0.063}$	0.3086 ± 0.0063	0.3082 ± 0.0062
σ_8	$0.818^{+0.031}_{-0.027}$	$0.964^{+0.10}_{-0.045}$	$0.955^{+0.10}_{-0.042}$	0.811 ± 0.011	0.8114 ± 0.0091
χ^2_{\min}	1457.48	2761.04	2770.34	4231.80	4240.63
$\Delta\chi^2_{\min}$	-12.45	-4.76	-4.37	-8.44	-8.63
DIC	1471.29	2815.91	2824.51	4289.09	4297.22
Δ DIC	-6.82	-2.02	-1.94	-3.24	-3.98
AIC	1471.48	2821.04	2830.34	4291.80	4300.63
Δ AIC	-6.45	+1.24	+1.63	-2.44	-2.63

tions to well within 1σ , and we expect the same for the derived parameters, as we now show. For the derived parameter H_0 , $68.05 \pm 0.38 \text{ km s}^{-1} \text{Mpc}^{-1}$ in the Λ CDM model is the largest value and $67.80 \pm 0.64 \text{ km s}^{-1} \text{Mpc}^{-1}$ in the w_0w_a CDM parametrization is the smallest, giving a difference of 0.34σ . The Λ CDM model has the smallest $\Omega_m = 0.3059 \pm 0.0050$ and the w_0w_a CDM parametrization has the largest $\Omega_m = 0.3094 \pm 0.0063$ which differ from each other by 0.44σ while the Λ CDM model smallest $\sigma_8 = 0.8077 \pm 0.0057$ and the w_0w_2 CDM parametrization largest $\sigma_8 = 0.8125 \pm 0.0091$ differ by 0.45σ . In the $A_L = 1$ case the P18+lensing+non-CMB data compilation provides reasonably model-independent parameter constraints, with the largest difference being the 0.52σ for $\Omega_c h^2$.

For the A_L -varying dark energy models and parametrizations, where we include the XCDM+ A_L case, the largest model-to-model differences for the six common model parameters are as follows. For $\Omega_b h^2$ the largest is 0.02263 ± 0.00014 in the XCDM+ A_L parametrization and the smallest is 0.02255 ± 0.00015 in the w_0w_2 CDM+ A_L or w_0w_p CDM+ A_L or $w_0w_1w_2$ CDM+ A_L parametrization, resulting in a difference of 0.39σ . For $\Omega_c h^2$ the smallest is 0.1168 ± 0.0011 in the XCDM+ A_L parametrization and the largest is 0.1179 ± 0.0012 in the w_0w_2 CDM+ A_L case, resulting in a difference of 0.68σ . For $100\theta_{\text{MC}}$, the XCDM+ A_L parametrization $100\theta_{\text{MC}} = 1.04126 \pm 0.00030$ is the largest and the w_0w_p CDM+ A_L or $w_0w_1w_2$ CDM+ A_L case $100\theta_{\text{MC}} = 1.04113 \pm 0.00030$ is the smallest, giving a

Table 5. Mean and 68% (or 95%) confidence limits of flat w_0w_pp CDM+ A_L model parameters from non-CMB, P18, P18+lensing, P18+non-CMB, and P18+lensing+non-CMB data. H_0 has units of $\text{km s}^{-1} \text{Mpc}^{-1}$. We also list the values of χ^2_{\min} , DIC, and AIC and the differences with respect to the values in the flat Λ CDM model for the same dataset, denoted by $\Delta\chi^2_{\min}$, Δ DIC, and Δ AIC, respectively.

Parameter	Non-CMB	P18	P18+lensing	P18+non-CMB	P18+lensing+non-CMB
$\Omega_b h^2$	0.0308 ± 0.0044	0.02258 ± 0.00017	0.02250 ± 0.00017	0.02263 ± 0.00015	0.02255 ± 0.00015
$\Omega_c h^2$	$0.1014^{+0.0073}_{-0.012}$	0.1182 ± 0.0015	0.1185 ± 0.0015	0.1177 ± 0.0012	0.1178 ± 0.0012
$100\theta_{\text{MC}}$	$1.0228^{+0.0097}_{-0.011}$	1.04113 ± 0.00032	1.04108 ± 0.00032	1.04118 ± 0.00031	1.04113 ± 0.00030
τ	0.0540	$0.0495^{+0.0089}_{-0.0077}$	$0.0494^{+0.0087}_{-0.0074}$	$0.0481^{+0.0088}_{-0.0074}$	$0.0481^{+0.0087}_{-0.0073}$
n_s	0.9655	0.9705 ± 0.0049	0.9690 ± 0.0048	0.9718 ± 0.0043	0.9705 ± 0.0042
$\ln(10^{10} A_s)$	$3.52 \pm 0.26 (> 3.06)$	$3.030^{+0.019}_{-0.016}$	$3.029^{+0.019}_{-0.016}$	$3.026^{+0.018}_{-0.015}$	$3.025^{+0.018}_{-0.015}$
A_L	...	$1.165^{+0.063}_{-0.088}$	$1.047^{+0.039}_{-0.058}$	1.184 ± 0.064	1.072 ± 0.038
w_0	$-0.865^{+0.048}_{-0.041}$	$-1.16^{+0.44}_{-0.66}$	$-1.24^{+0.37}_{-0.63}$	$-0.916^{+0.032}_{-0.043}$	$-0.917^{+0.032}_{-0.042}$
w_p	$-0.25^{+0.95}_{-0.23}$	$-0.81^{+0.82}_{-2.1}$	$-0.8 \pm 1.3 (< 1.41)$	$-1.29^{+1.1}_{-0.69}$	$-1.34^{+1.1}_{-0.69}$
p	$2.5 \pm 1.1 (> 0.454)$	$2.0^{+1.3}_{-1.5}$	$2.0 \pm 1.1 (> 0.269)$	$2.8 \pm 0.9 (> 0.980)$	$2.8 \pm 0.9 (> 1.01)$
$w_0 + w_p$	$-1.11^{+0.96}_{-0.19}$	$-1.97^{+1.5}_{-0.95}$	$-2.0^{+1.4}_{-1.1}$	$-2.20^{+1.1}_{-0.62}$	$-2.26^{+1.2}_{-0.63}$
H_0	69.7 ± 2.4	$77^{+20}_{-8} (> 54.7)$	$80 \pm 13 (> 57.7)$	67.94 ± 0.65	67.91 ± 0.64
Ω_m	$0.273^{+0.011}_{-0.017}$	$0.261^{+0.030}_{-0.012}$	$0.241^{+0.023}_{-0.19}$	0.3054 ± 0.0063	0.3059 ± 0.0063
σ_8	$0.818^{+0.031}_{-0.027}$	$0.874^{+0.16}_{-0.080}$	$0.899^{+0.15}_{-0.067}$	0.795 ± 0.012	0.797 ± 0.012
χ^2_{\min}	1457.48	2755.89	2770.20	4221.77	4237.05
$\Delta\chi^2_{\min}$	-12.45	-9.91	-4.51	-18.47	-12.21
DIC	1471.29	2812.89	2825.96	4282.60	4295.60
Δ DIC	-6.82	-5.04	-0.49	-9.73	-5.60
AIC	1471.48	2817.89	2832.20	4282.60	4299.05
Δ AIC	-6.45	-1.91	+3.50	-10.47	-4.21

difference of 0.31σ . For τ the largest difference is 0.16σ between the Λ CDM+ A_L model smallest $\tau = 0.0477 \pm 0.0086$ and the XCDM+ A_L parametrization largest $\tau = 0.0496 \pm 0.0083$, while for n_s the largest difference is 0.48σ between the XCDM+ A_L parametrization largest $n_s = 0.9733 \pm 0.0040$ and the w_0w_pp CDM+ A_L case smallest $n_s = 0.9705 \pm 0.0042$. For $\ln(10^{10} A_s)$, the Λ CDM+ A_L model smallest $\ln(10^{10} A_s) = 3.024 \pm 0.018$ and the XCDM+ A_L case largest $\ln(10^{10} A_s) = 3.026 \pm 0.017$ differ at 0.08σ . For the derived parameters, the largest $H_0 = 68.45 \pm 0.42 \text{ km s}^{-1} \text{Mpc}^{-1}$ in the Λ CDM+ A_L model and the smallest $H_0 = 67.79 \pm 0.63 \text{ km s}^{-1} \text{Mpc}^{-1}$ in the XCDM+ A_L case differ at 0.87σ . The Λ CDM+ A_L model smallest $\Omega_m = 0.3005 \pm 0.0053$ and the w_0w_a CDM+ A_L case largest $\Omega_m = 0.3062 \pm 0.0064$ differ by 0.69σ while the XCDM+ A_L model smallest $\sigma_8 = 0.785 \pm 0.011$ and the w_0w_2 CDM+ A_L or w_0w_pp CDM or $w_0w_1w_2$ CDM parametrization largest $\sigma_8 = 0.797 \pm 0.012$ differ from each other by 0.74σ . The spread in parameter values across dark energy models and parametrizations, when measured using P18+lensing+non-CMB data, is a little larger when A_L is allowed to vary, compared to the $A_L = 1$ case. Among the six common primary parameters, the biggest spread, 0.68σ , is again in $\Omega_c h^2$, while the three derived parameters have larger spreads, ranging from 0.69σ to 0.87σ . Since these are all smaller than 1σ we conclude that even in the varying

Is excess smoothing of Planck data partially responsible for DE dynamics in $w(z)$ CDM? 17

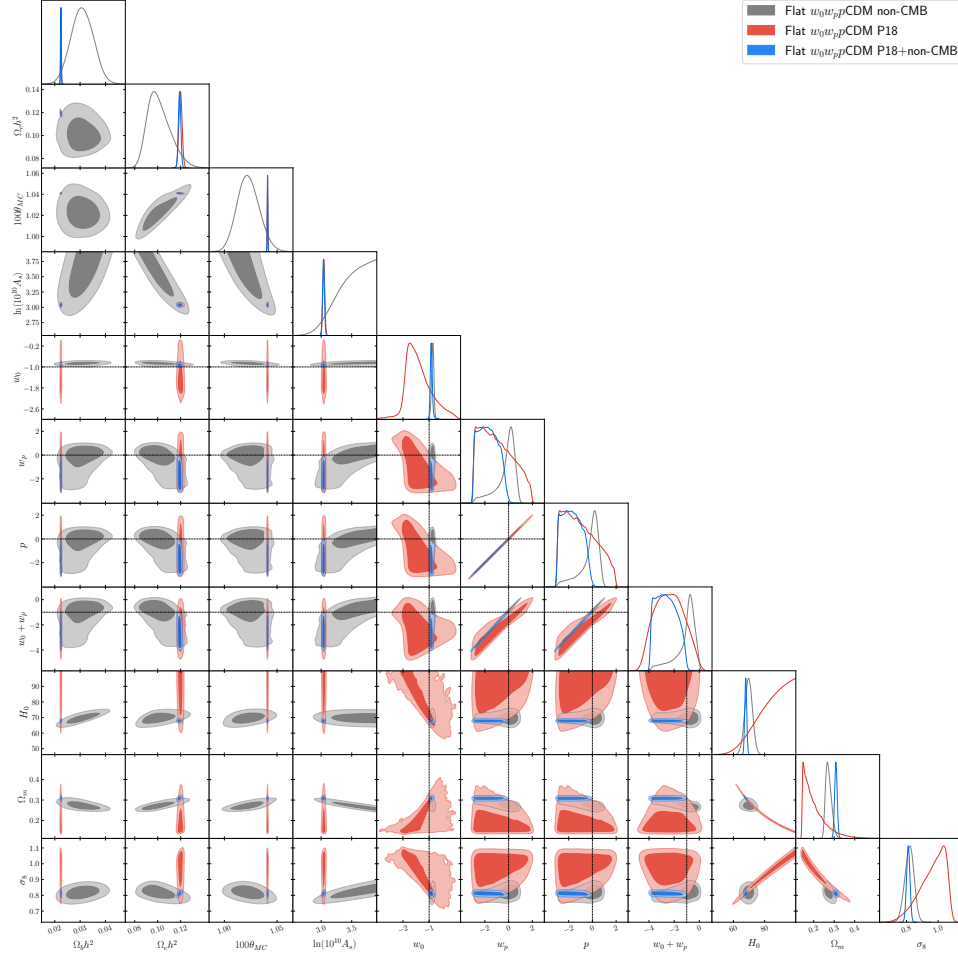


Fig. 7. One-dimensional likelihoods and 1σ and 2σ likelihood confidence contours of flat $w_0 w_p$ CDM model parameters favored by non-CMB, P18, and P18+non-CMB datasets. We do not show τ and n_s , which are fixed in the non-CMB data analysis.

A_L case P18+lensing+non-CMB data provide reasonably model-independent cosmological parameter measurements.

For all the $A_L = 1$ and A_L -varying dark energy models and parametrizations together, but excluding the XCDM case with $A_L = 1$, the largest model-to-model differences for the six common model parameters are as follows. For $\Omega_b h^2$, the largest 0.02263 ± 0.00014 in the XCDM+ A_L case and the smallest 0.02244 ± 0.00014 in the $w_0 w_a$ CDM or $w_0 w_2$ CDM parametrization have a difference of 0.96σ . For $\Omega_c h^2$ the smallest is 0.1168 ± 0.0011 in the XCDM+ A_L case and the largest is 0.11917 ± 0.00099 in the $w_0 w_2$ CDM parametrization, resulting in a difference of 1.60σ . For $100\theta_{MC}$, the XCDM+ A_L case $100\theta_{MC} = 1.04126 \pm 0.00030$ is the largest

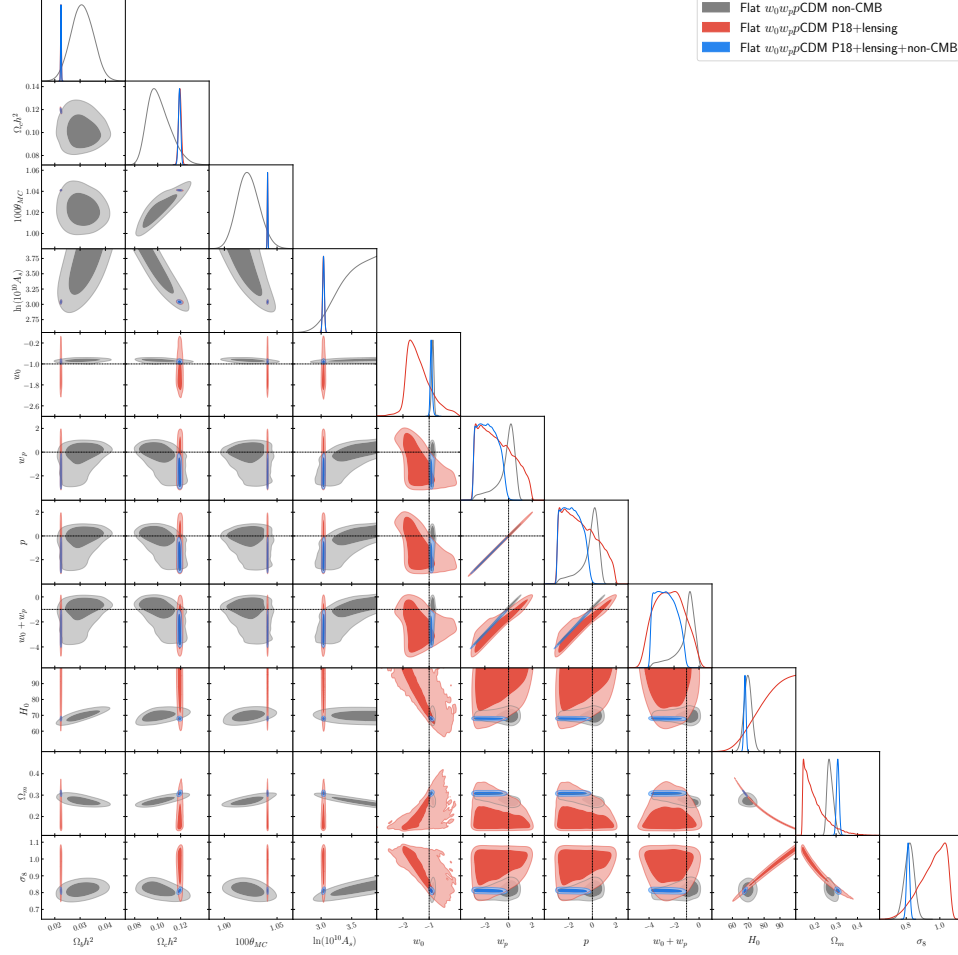


Fig. 8. One-dimensional likelihoods and 1σ and 2σ likelihood confidence contours of flat $w_0 w_p$ Λ CDM model parameters favored by non-CMB, P18+lensing, P18+lensing+non-CMB datasets. We do not show τ and n_s , which are fixed in the non-CMB data analysis.

and the $w_0 w_2$ CDM parametrization $100\theta_{MC} = 1.04098 \pm 0.00030$ is the smallest, and these have a difference of 0.66σ . For τ the largest difference is 0.82σ between the Λ CDM model largest $\tau = 0.0569 \pm 0.0071$ and the Λ CDM+ A_L model smallest $\tau = 0.0477 \pm 0.0086$, while for n_s the largest difference is 1.18σ between the XCDM+ A_L case largest $n_s = 0.9733 \pm 0.0040$ and the $w_0 w_2$ CDM case smallest $n_s = 0.9668 \pm 0.0038$. For $\ln(10^{10} A_s)$, the Λ CDM model largest $\ln(10^{10} A_s) = 3.046 \pm 0.014$ and the Λ CDM+ A_L model smallest $\ln(10^{10} A_s) = 3.024 \pm 0.018$ differ at 0.96σ . For the derived parameters, the largest $H_0 = 68.45 \pm 0.42 \text{ km s}^{-1} \text{ Mpc}^{-1}$ in the Λ CDM+ A_L model and the smallest $H_0 = 67.79 \pm 0.63 \text{ km s}^{-1} \text{ Mpc}^{-1}$ in the XCDM+ A_L case differ by 0.87σ . The Λ CDM+ A_L model smallest $\Omega_m = 0.3005 \pm 0.0053$ and the

Is excess smoothing of Planck data partially responsible for DE dynamics in $w(z)$ CDM? 19

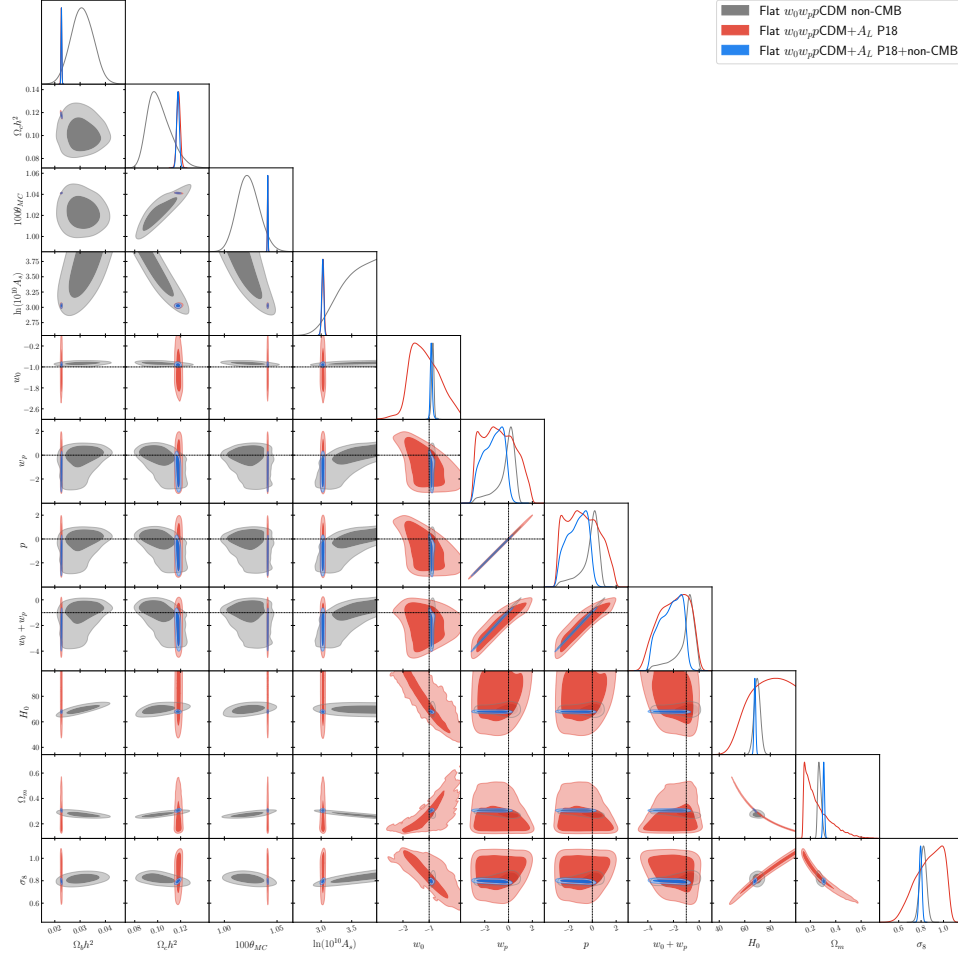


Fig. 9. One-dimensional likelihoods and 1σ and 2σ likelihood confidence contours of flat $w_0 w_p$ CDM + A_L model parameters favored by non-CMB, P18, and P18+non-CMB datasets. We do not show τ and n_s , which are fixed in the non-CMB data analysis.

$w_0 w_a$ CDM case largest $\Omega_m = 0.3094 \pm 0.0063$ have the largest difference of 1.08σ while the Λ CDM + A_L case smallest $\sigma_8 = 0.785 \pm 0.011$ and the $w_0 w_2$ CDM model parametrization largest $\sigma_8 = 0.8125 \pm 0.0091$ differ by 1.93σ . The parameter value differences are larger when we compare across all the $A_L = 1$ and varying A_L cases, caused by the somewhat significant changes in some parameter values when the lensing consistency parameter is allowed to vary, compared to the $A_L = 1$ case values.

As described above, the significance of the difference between the largest and smallest H_0 values are 0.34σ (when $A_L = 1$), 0.87σ (when A_L varies), and 0.87σ (overall), indicating that for these models P18+lensing+non-CMB data provide a

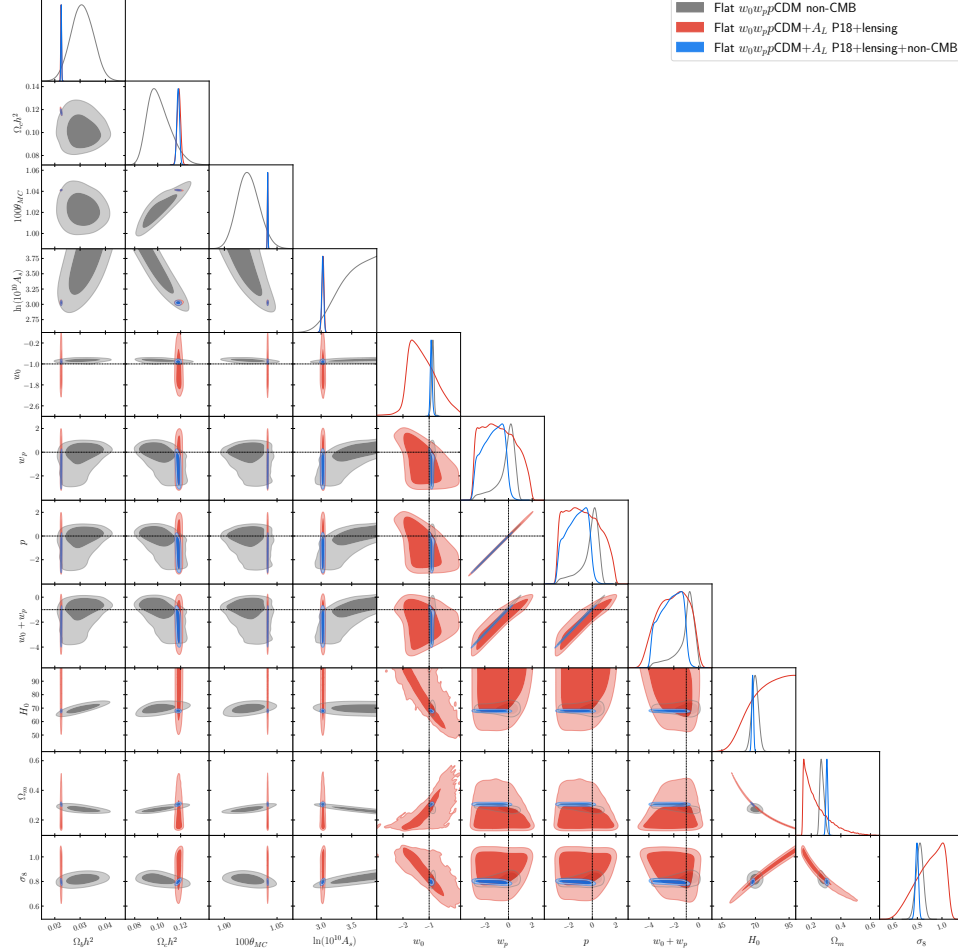


Fig. 10. One-dimensional likelihoods and 1σ and 2σ likelihood confidence contours of flat $w_0 w_p \text{CDM} + A_L$ model parameters favored by non-CMB, P18+lensing, P18+lensing+non-CMB datasets. We do not show τ and n_s , which are fixed in the non-CMB data analysis.

reasonably model-independent H_0 value, which may be summarized as $H_0 = 68.1 \pm 0.9 \text{ km s}^{-1} \text{ Mpc}^{-1}$, where the central value is the average of the smallest and largest values and the error bar is half of the spread between the largest upper 1σ value and the smallest lower 1σ value. This summary values agrees with the median statistics result $H_0 = 68 \pm 2.8 \text{ km s}^{-1} \text{ Mpc}^{-1}$.^{93–95} It also agrees with some local measurements including the summary value of Ref. 79 $H_0 = 69.25 \pm 2.42 \text{ km s}^{-1} \text{ Mpc}^{-1}$ from a joint analysis of $H(z)$, BAO, Pantheon+ SNIa, quasar angular size, reverberation-measured Mg II and C IV quasar, and 118 Amati correlation gamma-ray burst data, and the local $H_0 = 69.03 \pm 1.75 \text{ km s}^{-1} \text{ Mpc}^{-1}$ from JWST TRGB+JAGB and SNIa data,⁹⁶ but is smaller than the local $H_0 = 73.04 \pm 1.04 \text{ km s}^{-1} \text{ Mpc}^{-1}$ measured

Is excess smoothing of Planck data partially responsible for DE dynamics in $w(z)$ CDM? 21

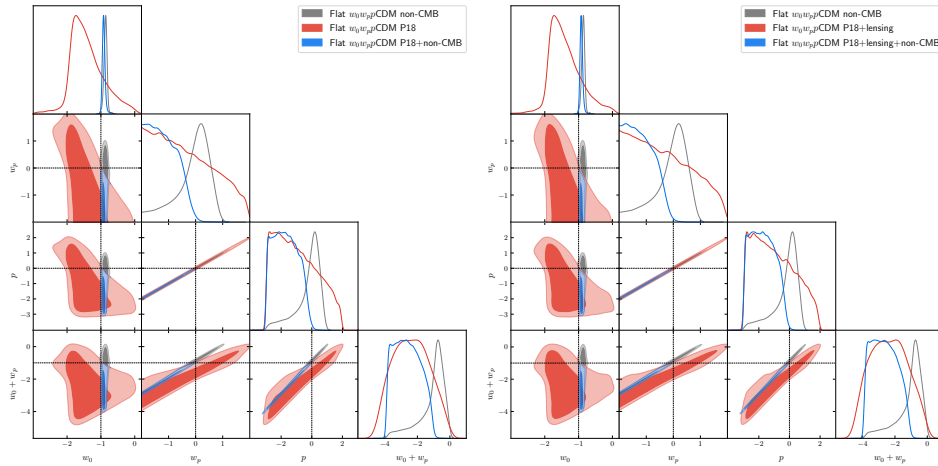


Fig. 11. One-dimensional likelihoods and 1σ and 2σ likelihood confidence contours of w_0 , w_p , p , and $w_0 + w_p$ parameters in the flat w_0w_p CDM parametrization favored by (left) non-CMB, P18, and P18+non-CMB datasets, and (right) non-CMB, P18+lensing, and P18+lensing+non-CMB datasets.

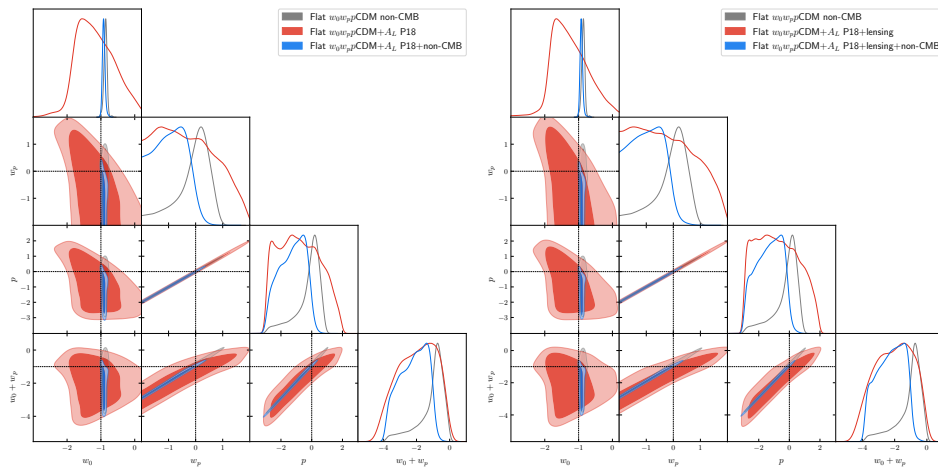


Fig. 12. One-dimensional likelihoods and 1σ and 2σ likelihood confidence contours of w_0 , w_p , p , and $w_0 + w_p$ parameters in the flat w_0w_p CDM+ A_L model favored by (left) non-CMB, P18, and P18+non-CMB datasets, and (right) non-CMB, P18+lensing, and P18+lensing+non-CMB datasets.

using Cepheids and SNIa data,⁹⁷ also see Refs. 98,99.

Table 8 lists the current low-redshift, w_0 , and high-redshift, $w(z \rightarrow \infty)$, values of the dynamical dark energy equation of state parameter, $w(z)$, as well as the lensing consistency parameter, A_L , values, measured using P18+lensing+non-CMB data, in a number of dynamical dark energy parametrizations. The XCDM+ A_L

Table 6. Mean and 68% (or 95%) confidence limits of flat $w_0w_1w_2$ CDM model parameters from non-CMB, P18, P18+lensing, P18+non-CMB, and P18+lensing+non-CMB data. H_0 has units of $\text{km s}^{-1} \text{Mpc}^{-1}$. We also list the values of χ^2_{\min} , DIC, and AIC and the differences with respect to the values in the flat Λ CDM model for the same dataset, denoted by $\Delta\chi^2_{\min}$, Δ DIC, and Δ AIC, respectively.

Parameter	Non-CMB	P18	P18+lensing	P18+non-CMB	P18+lensing+non-CMB
$\Omega_b h^2$	0.0311 ± 0.0043	0.02240 ± 0.00015	0.02244 ± 0.00015	0.02244 ± 0.00014	0.02245 ± 0.00014
$\Omega_c h^2$	$0.0999^{+0.0064}_{-0.012}$	0.1198 ± 0.0014	0.1192 ± 0.0012	0.1191 ± 0.0011	0.11912 ± 0.00099
$100\theta_{\text{MC}}$	$1.0214^{+0.0092}_{-0.012}$	1.04094 ± 0.00031	1.04101 ± 0.00031	1.04100 ± 0.00030	1.04099 ± 0.00030
τ	0.0540	0.0540 ± 0.0078	0.0520 ± 0.0075	0.0524 ± 0.0077	0.0528 ± 0.0074
n_s	0.9656	0.9656 ± 0.0044	0.9671 ± 0.0042	0.9671 ± 0.0040	0.9670 ± 0.0038
$\ln(10^{10}A_s)$	$3.56 \pm 0.26 (> 3.06)$	3.043 ± 0.016	3.037 ± 0.015	3.038 ± 0.016	3.039 ± 0.014
w_0	$-0.920^{+0.078}_{-0.088}$	$-1.19^{+0.39}_{-0.59}$	$-1.18^{+0.40}_{-0.59}$	$-0.928^{+0.078}_{-0.094}$	$-0.929^{+0.077}_{-0.095}$
w_1	$0.54^{+0.83}_{-0.66}$	$-1.1 \pm 1.3 (< 1.29)$	$-1.1 \pm 1.3 (< 1.36)$	$0.25^{+0.86}_{-0.47}$	$0.27^{+0.87}_{-0.45}$
w_2	$-0.8^{+1.1}_{-1.4}$	$-0.9 \pm 1.4 (< 1.51)$	$-1.1 \pm 1.3 (< 1.54)$	$-1.5 \pm 1.1 (< 0.732)$	$-1.5 \pm 1.1 (< 0.709)$
$w_0 + w_1 + w_2$	$-1.21^{+0.78}_{-0.56}$	$-3.3^{+1.6}_{-1.5}$	$-3.1^{+1.7}_{-1.4}$	$-2.14^{+0.42}_{-0.73}$	$-2.15^{+0.40}_{-0.71}$
H_0	69.8 ± 2.3	$84 \pm 11 (> 63.4)$	$83 \pm 11 (> 63.6)$	67.92 ± 0.64	67.92 ± 0.64
Ω_m	$0.2703^{+0.0093}_{-0.018}$	$0.217^{+0.018}_{-0.074}$	$0.218^{+0.019}_{-0.075}$	0.3084 ± 0.0063	0.3084 ± 0.0063
σ_8	$0.823^{+0.031}_{-0.026}$	$0.950^{+0.12}_{-0.053}$	$0.939^{+0.11}_{-0.052}$	0.812 ± 0.011	0.8118 ± 0.0090
χ^2_{\min}	1457.13	2760.82	2770.51	4232.22	4240.75
$\Delta\chi^2_{\min}$	-12.80	-4.98	-4.20	-8.02	-8.51
DIC	1471.28	2815.65	2824.37	4289.73	4298.65
Δ DIC	-6.83	-2.28	-2.08	-2.60	-2.55
AIC	1471.13	2820.82	2830.51	4292.22	4300.75
Δ AIC	-6.83	+1.02	+1.80	-2.02	-2.51

parametrization value is from Ref. 58 and the w_0w_a CDM ($+A_L$) values are from Refs. 19, 50.

In the XCDM parametrization P18+lensing data favor phantom-like ($w < -1$) dynamical dark energy while non-CMB data favor quintessence-like ($w > -1$) behavior,⁵⁸ so much so that the cosmological constraints from these two datasets are inconsistent at 3.6σ , thus ruling out the XCDM parametrization at $> 3\sigma$.⁵⁸ Allowing A_L to be an additional free parameter to be determined from data, so now considering the XCDM+ A_L dynamical dark energy parametrization, somewhat reconciles the P18+lensing and the non-CMB constraints, to 2.4σ inconsistency, and a joint P18+lensing+non-CMB data analysis then indicates a 1.3σ preference for a quintessence-like $w_0 = -0.968 \pm 0.024$, but also requires $A_L = 1.101 \pm 0.037$, > 1 at 2.73σ significance.⁵⁸ As noted above, non-CMB data are more effective at constraining $w(z)$ than are P18 or P18+lensing data. In the XCDM parametrization, non-CMB data results in $w_0 = -0.853^{+0.043}_{-0.033}$, while P18+lensing data give $w_0 = -1.55 \pm 0.26$ ($w_0 = -1.34^{+0.26}_{-0.51}$) when $A_L = 1$ (when A_L is allowed to vary and determined from P18+lensing data to be 1.054 ± 0.055). This shift in w_0 towards quintessence-like behavior when A_L is allowed to vary away from unity suggests that the observed excess smoothing of some of the Planck CMB multipoles (relative to what is expected in the best-fit Planck cosmological model) is partially responsible for the phantom-like behavior seen in the XCDM parametrization when

Is excess smoothing of Planck data partially responsible for DE dynamics in $w(z)$ CDM? 23

Table 7. Mean and 68% (or 95%) confidence limits of flat $w_0w_1w_2$ CDM+ A_L model parameters from non-CMB, P18, P18+lensing, P18+non-CMB, and P18+lensing+non-CMB data. H_0 has units of $\text{km s}^{-1} \text{Mpc}^{-1}$. We also list the values of χ^2_{\min} , DIC, and AIC and the differences with respect to the values in the flat Λ CDM model for the same dataset, denoted by $\Delta\chi^2_{\min}$, Δ DIC, and Δ AIC, respectively.

Parameter	Non-CMB	P18	P18+lensing	P18+non-CMB	P18+lensing+non-CMB
$\Omega_b h^2$	0.0311 ± 0.0043	0.02259 ± 0.00017	0.02249 ± 0.00017	0.02263 ± 0.00016	0.02255 ± 0.00015
$\Omega_c h^2$	$0.0999^{+0.0064}_{-0.012}$	0.1181 ± 0.0015	0.1185 ± 0.0015	0.1176 ± 0.0012	0.1178 ± 0.0012
$100\theta_{\text{MC}}$	$1.0214^{+0.0092}_{-0.012}$	1.04115 ± 0.00033	1.04107 ± 0.00033	1.04117 ± 0.00031	1.04113 ± 0.00030
τ	0.0540	$0.0494^{+0.0087}_{-0.0075}$	$0.0491^{+0.0086}_{-0.0074}$	$0.0482^{+0.0085}_{-0.0072}$	$0.0481^{+0.0085}_{-0.0074}$
n_s	0.9656	0.9706 ± 0.0049	0.9688 ± 0.0048	0.9718 ± 0.0043	0.9706 ± 0.0042
$\ln(10^{10} A_s)$	$3.56 \pm 0.26 (> 3.06)$	$3.030^{+0.018}_{-0.016}$	$3.029^{+0.018}_{-0.016}$	$3.026^{+0.017}_{-0.015}$	$3.025^{+0.017}_{-0.015}$
A_L	...	$1.158^{+0.060}_{-0.087}$	$1.040^{+0.041}_{-0.053}$	1.185 ± 0.064	$1.073^{+0.036}_{-0.040}$
w_0	$-0.920^{+0.078}_{-0.088}$	$-0.99^{+0.52}_{-0.67}$	$-1.06^{+0.50}_{-0.66}$	$-0.940^{+0.082}_{-0.10}$	$-0.943^{+0.083}_{-0.095}$
w_1	$0.54^{+0.83}_{-0.66}$	$-0.8 \pm 1.3 (< 1.51)$	$-0.9 \pm 1.4 (< 1.51)$	$0.29^{+0.97}_{-0.54}$	$0.31^{+0.94}_{-0.54}$
w_2	$-0.8^{+1.1}_{-1.4}$	$-0.8 \pm 1.4 (< 1.55)$	$-0.8 \pm 1.4 (< 1.56)$	$-1.2 \pm 1.2 (< 1.18)$	$-1.2 \pm 1.2 (< 1.08)$
$w_0 + w_1 + w_2$	$-1.21^{+0.78}_{-0.56}$	$-2.6^{+1.9}_{-1.1}$	$-2.7^{+1.8}_{-1.3}$	$-1.82^{+0.47}_{-0.82}$	$-1.88^{+0.50}_{-0.79}$
H_0	69.8 ± 2.3	$77^{+20}_{-10} (> 54.9)$	$79 \pm 13 (> 57.6)$	67.96 ± 0.65	67.96 ± 0.64
Ω_m	$0.2703^{+0.0093}_{-0.018}$	$0.267^{+0.036}_{-0.13}$	$0.249^{+0.030}_{-0.13}$	0.3051 ± 0.0064	0.3054 ± 0.0063
σ_8	$0.823^{+0.031}_{-0.026}$	$0.868^{+0.16}_{-0.088}$	$0.891^{+0.14}_{-0.078}$	0.795 ± 0.012	0.797 ± 0.012
χ^2_{\min}	1457.13	2755.91	2770.25	4222.96	4237.21
$\Delta\chi^2_{\min}$	-12.80	-9.89	-4.46	-17.28	-12.05
DIC	1471.28	2813.02	2832.25	4282.32	4296.50
Δ DIC	-6.83	-4.91	-0.17	-10.01	-4.70
AIC	1471.13	2817.91	2832.25	4284.96	4299.21
Δ AIC	-6.83	-1.89	+3.54	-9.28	-4.05

Table 8. Mean and 68% confidence limits of w_0 , $w(z \rightarrow \infty)$, and A_L values in dynamical dark energy parametrizations for P18+lensing+non-CMB data. Significances shown in parentheses for w_0 and $w(z \rightarrow \infty)$ indicate how much larger (smaller) than -1 they are when the following index is qu (ph), while those for A_L indicate how much larger than unity it is. We do not list values for the XCDM parameterization as that is observationally inconsistent at $> 3\sigma$ significance with these data.

Parametrization	w_0	$w(z \rightarrow \infty)$	A_L
XCDM+ A_L	$-0.968 \pm 0.024 (1.33\sigma \text{ qu})$	$-0.968 \pm 0.024 (1.33\sigma \text{ qu})$	$1.101 \pm 0.037 (2.73\sigma)$
w_0w_a CDM	$-0.850 \pm 0.059 (2.54\sigma \text{ qu})$	$-1.44^{+0.20}_{-0.17} (2.20\sigma \text{ ph})$	1
w_0w_a CDM+ A_L	$-0.879 \pm 0.060 (2.02\sigma \text{ qu})$	$-1.27^{+0.20}_{-0.17} (1.35\sigma \text{ ph})$	$1.078^{+0.036}_{-0.040} (1.95\sigma)$
w_0w_2 CDM	$-0.898 \pm 0.040 (2.55\sigma \text{ qu})$	$-2.02^{+0.47}_{-0.37} (2.17\sigma \text{ ph})$	1
w_0w_2 CDM+ A_L	$-0.908 \pm 0.040 (2.30\sigma \text{ qu})$	$-1.69^{+0.45}_{-1.2} (1.53\sigma \text{ ph})$	$1.072 \pm 0.038 (1.89\sigma)$
w_0w_p pCDM	$-0.916^{+0.031}_{-0.045} (1.87\sigma \text{ qu})$	$-1.73^{+0.48}_{-1.2} (1.52\sigma \text{ ph})$	1
w_0w_p pCDM+ A_L	$-0.917^{+0.032}_{-0.042} (1.98\sigma \text{ qu})$	$-2.26^{+1.2}_{-0.63} (1.05\sigma \text{ ph})$	$1.072 \pm 0.038 (1.89\sigma)$
$w_0w_1w_2$ CDM	$-0.929^{+0.077}_{-0.095} (0.747\sigma \text{ qu})$	$-2.15^{+0.40}_{-0.71} (2.88\sigma \text{ ph})$	1
$w_0w_1w_2$ CDM+ A_L	$-0.943^{+0.083}_{-0.095} (0.600\sigma \text{ qu})$	$-1.88^{+0.50}_{-0.79} (1.76\sigma \text{ ph})$	$1.073^{+0.036}_{-0.040} (1.83\sigma)$

P18+lensing data are used in the analysis.

When $w(z)$ is parametrized using more than one parameter, such as w_0 and w_a in the w_0w_a CDM parametrization where $w(z) = w_0 + w_az/(1+z)$, there is more freedom so the situation differs a bit from the XCDM case discussed in the previous

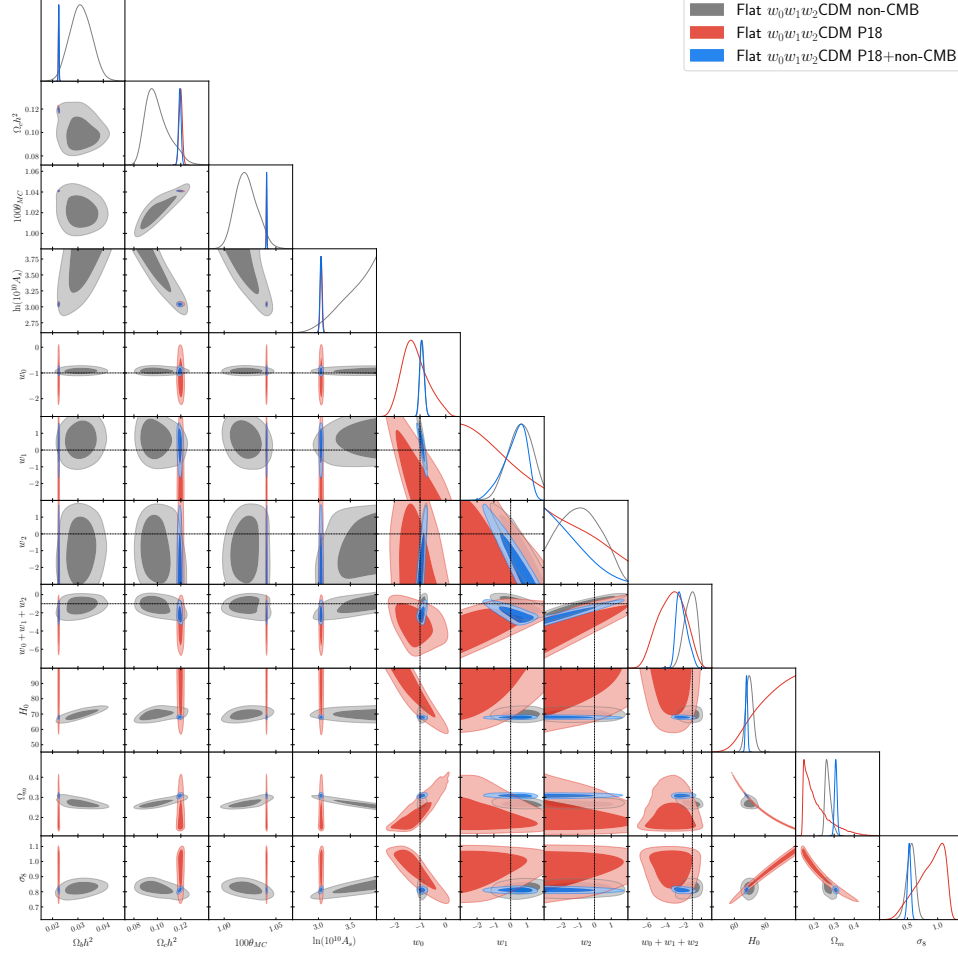


Fig. 13. One-dimensional likelihoods and 1σ and 2σ likelihood confidence contours of flat $w_0w_1w_2$ CDM model parameters favored by non-CMB, P18, and P18+non-CMB datasets. We do not show τ and n_s , which are fixed in the non-CMB data analysis.

paragraph. In the two and three parameter $w(z)$ cases we study the P18+lensing constraints and the non-CMB constraints are inconsistent at less than 3σ , even when $A_L = 1$, see Table 1 and the related discussion above; this differs from what happens in the XCDM case. However, allowing A_L to vary makes the P18+lensing constraints and the non-CMB constraints more consistent, which is similar to what happens in the XCDM case. In the w_0w_a CDM case, as discussed in Ref. 50, non-CMB data favor quintessence-like behavior, with $w_0 = -0.876 \pm 0.055$, while P18+lensing data favor phantom-like behavior, with $w_0 = -1.24^{+0.44}_{-0.56}$ when $A_L = 1$ and $w_0 = -1.14^{+0.48}_{-0.68}$ with $A_L = 1.046^{+0.038}_{-0.057}$. In this case P18+lensing+non-CMB data favors quintessence-like $w_0 = -0.850 \pm 0.059$ at 2.54σ ($w_0 = -0.879 \pm 0.060$ at 2.02σ)

Is excess smoothing of Planck data partially responsible for DE dynamics in $w(z)$ CDM? 25

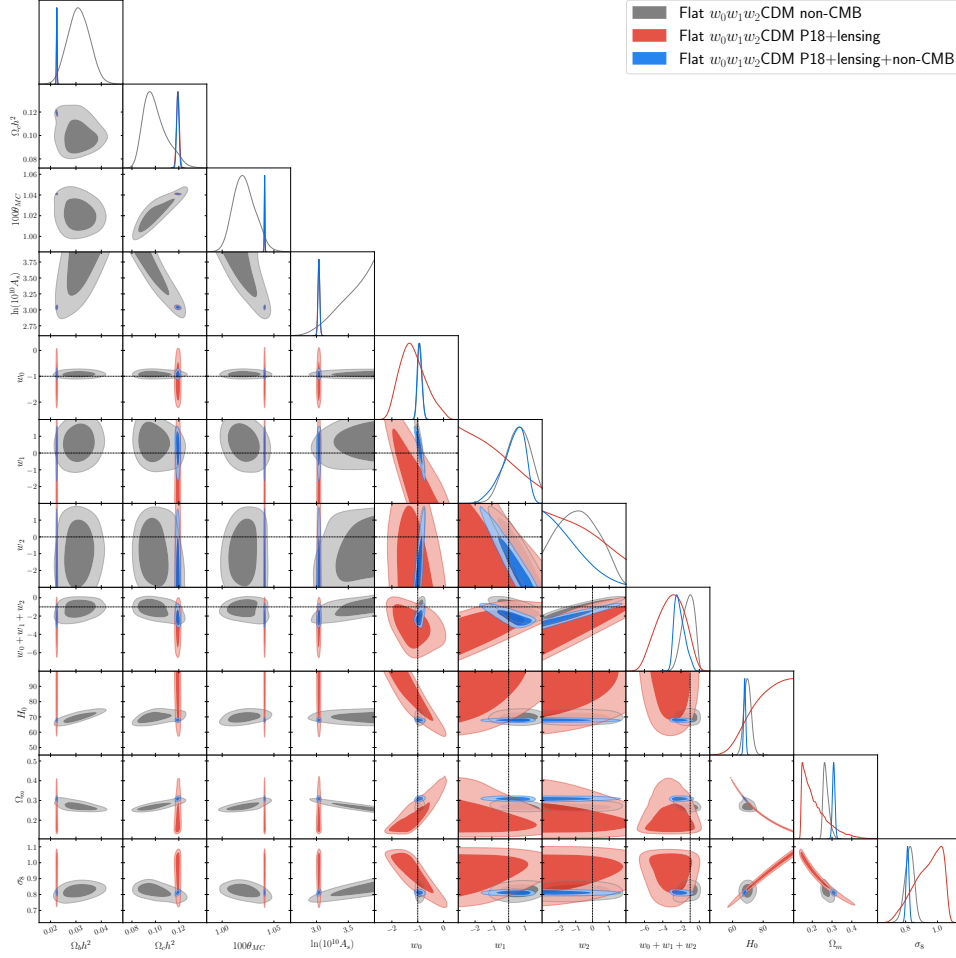


Fig. 14. One-dimensional likelihoods and 1σ and 2σ likelihood confidence contours of flat $w_0w_1w_2$ CDM model parameters favored by non-CMB, P18+lensing, P18+lensing+non-CMB datasets. We do not show τ and n_s , which are fixed in the non-CMB data analysis.

while favoring quintessence-like $w(z \rightarrow \infty) = w_0 + w_a = -1.44^{+0.20}_{-0.17}$ at 2.20σ when $A_L = 1$ ($w(z \rightarrow \infty) = -1.27^{+0.20}_{-0.17}$ at 1.35σ with $A_L = 1.078^{+0.036}_{-0.040}$, > 1 at 1.95σ), see discussion in Ref. 50.

Similar behavior is true for all the other dynamical dark energy parametrizations we study here, as can be seen from the numerical values listed in Table 8. Excluding Λ CDM+ A_L , from the results for the other four parametrizations listed in Table 8, when $A_L = 1$ $w(z \rightarrow \infty)$ is phantom-like at significance ranging from a low of 1.5σ to a high of 2.9σ (with three of the four parametrizations favoring phantom-like behavior at $> 2\sigma$), while when A_L is allowed to vary the support for phantom-like $w(z \rightarrow \infty)$ has reduced significance ranging from a low of 1.1σ to a high of 1.8σ

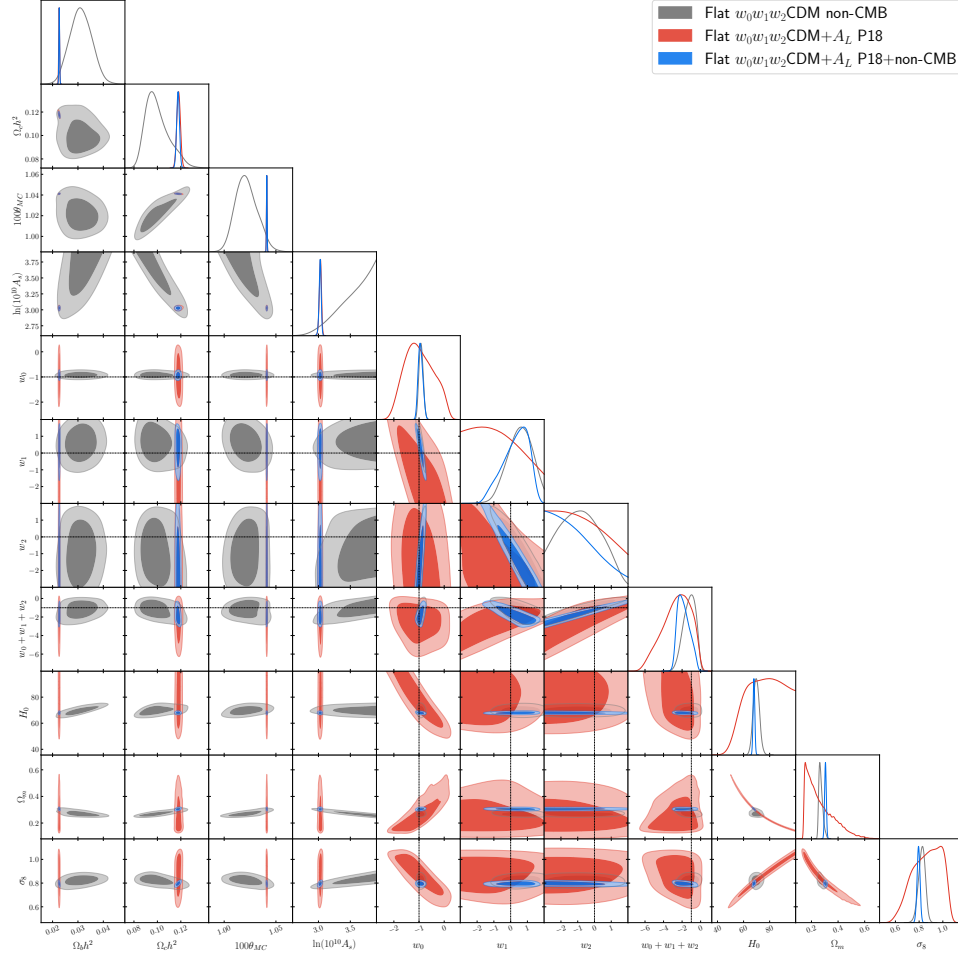


Fig. 15. One-dimensional likelihoods and 1σ and 2σ likelihood confidence contours of flat $w_0w_1w_2\text{CDM}+A_L$ model parameters favored by non-CMB, P18, and P18+non-CMB datasets. We do not show τ and n_s , which are fixed in the non-CMB data analysis.

(with none of the four parametrizations favoring phantom-like behavior at $> 2\sigma$).

We noted above that the two- and three-parameter $w(z)$ parametrizations have more flexibility than the XCDM parametrization and that at low and high redshift the two- and three-parameter parametrizations behave like XCDM parametrizations, but with two different constant w parameters. We also noted above that non-CMB data is more effective at constraining $w(z)$ since dark energy is not as important at the higher redshift, $z \sim 1100$, where CMB data is more sensitive. In the XCDM parametrization this means that in a joint analysis, like P18+lensing+non-CMB, which is only possible when A_L is allowed to vary (and which brings the P18+lensing constraints and the non-CMB constraints into less than 3σ inconsis-

Is excess smoothing of Planck data partially responsible for DE dynamics in $w(z)$ CDM? 27

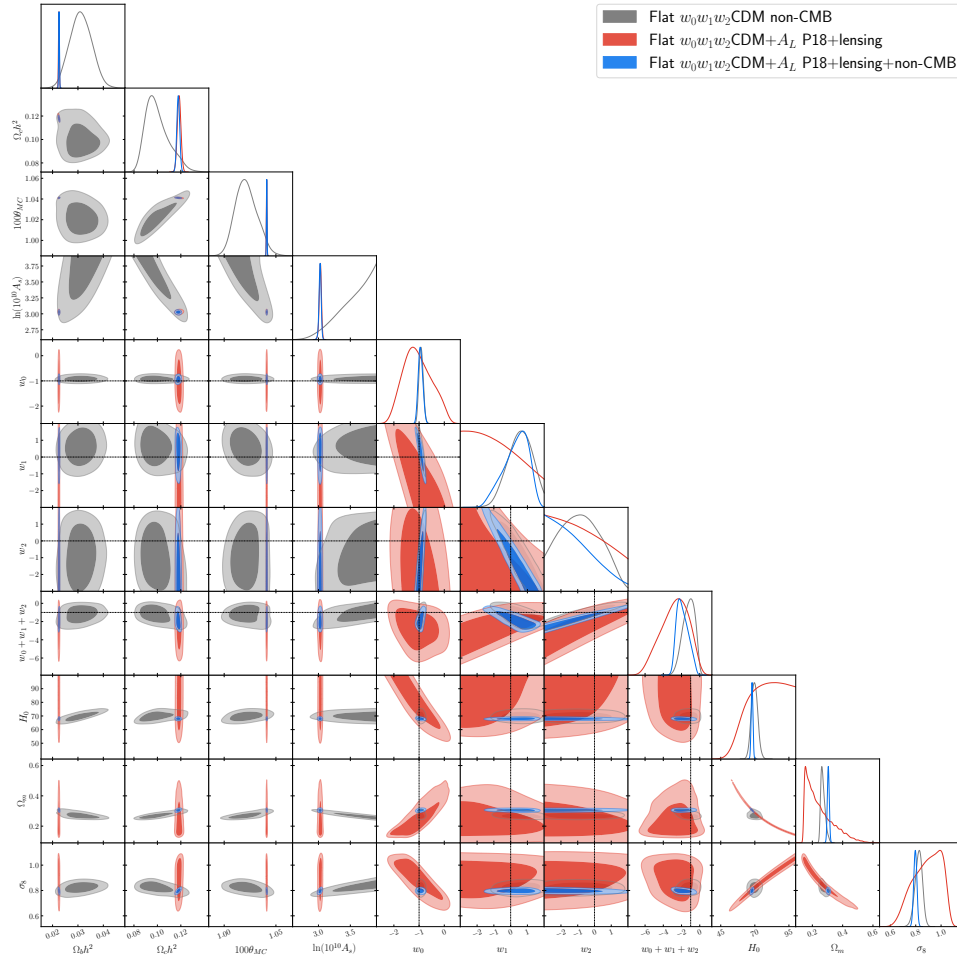


Fig. 16. One-dimensional likelihoods and 1σ and 2σ likelihood confidence contours of flat $w_0w_1w_2$ CDM+ A_L model parameters favored by non-CMB, P18+lensing, P18+lensing+non-CMB datasets. We do not show τ and n_s , which are fixed in the non-CMB data analysis.

tency), non-CMB data overwhelms P18+lensing data and results in quintessence-like dynamical dark energy, even though P18+lensing data favor phantom-like dynamical dark energy. In the two- and three-parameter $w(z)$ CDM parametrizations, $w(z)$ has more flexibility and while non-CMB data is able to ensure low-redshift w_0 values that are quintessence-like even in joint P18+lensing+non-CMB analyses, and also increase the P18+lensing data high-redshift $w(z \rightarrow \infty)$ values, they are unable to pull it into the more-physical quintessence-like regime, although in all cases they are able to reduce the evidence for phantom-like behavior to below 2σ .

In addition to what is established from the numerical results given in Table 1, we can see by comparing the corresponding panels in Figures 5 and 6, 11 and

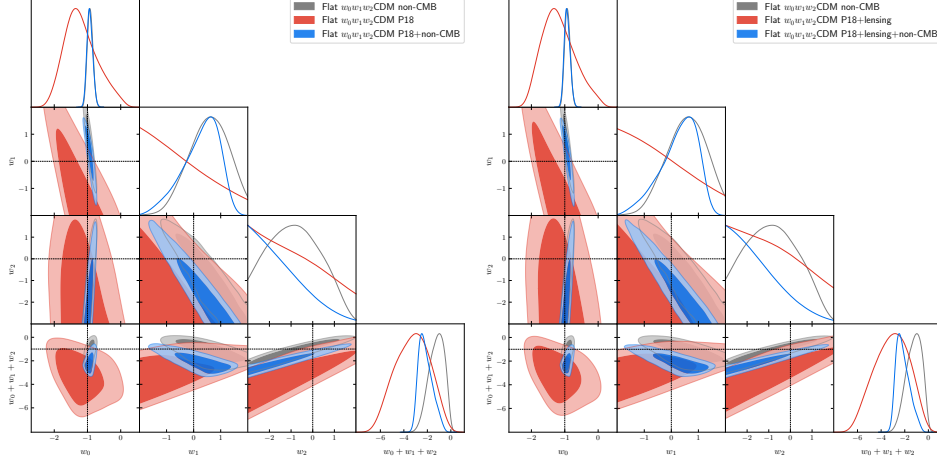


Fig. 17. One-dimensional likelihoods and 1σ and 2σ likelihood confidence contours of w_0 , w_1 , w_2 , and $w_0 + w_1 + w_2$ parameters in the flat $w_0w_1w_2$ CDM parametrization favored by (left) non-CMB, P18, and P18+non-CMB datasets, and (right) non-CMB, P18+lensing, and P18+lensing+non-CMB datasets.

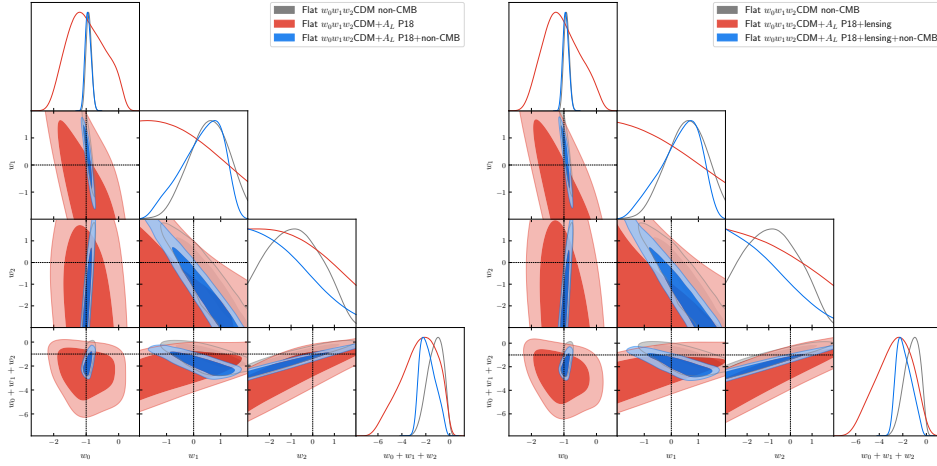


Fig. 18. One-dimensional likelihoods and 1σ and 2σ likelihood confidence contours of w_0 , w_1 , w_2 , and $w_0 + w_1 + w_2$ parameters in the flat $w_0w_1w_2$ CDM+ A_L parametrization favored by (left) non-CMB, P18, and P18+non-CMB datasets, and (right) non-CMB, P18+lensing, and P18+lensing+non-CMB datasets.

12, and 17 and 18, that allowing A_L to vary makes the P18 or the P18+lensing cosmological constraints more consistent with the non-CMB ones, compared to the $A_L = 1$ case. In what follows we focus on the P18+lensing data (red contours) and the non-CMB data (gray contours), those shown in the right-hand panels of these figures. In the $w_0 - w_2$ subpanels of the right-hand panels of Figures 5 and 6, for

Is excess smoothing of Planck data partially responsible for DE dynamics in $w(z)$ CDM? 29

the w_0w_2 CDM ($+A_L$) parametrizations, one sees when $A_L = 1$ (Fig. 5) the 2σ red and gray contours have some overlap, but when A_L is allowed to vary (Fig. 6) the 2σ grey contours has some overlap with the 1σ red contour and vice versa, with the gray and red 1σ contours almost touching. Similarly, in the $w_0 - w_p$, $w_0 - p$, and $w_p - p$ right-hand subpanels of Figures 11 and 12 for the w_0w_pp CDM ($+A_L$) parametrizations we see a significantly improved consistency between the red and gray contours when going from the $A_L = 1$ case to the varying A_L case; there is a degeneracy in the $w_p - p$ subpanels constraint contours that makes it difficult to examine this issue there. This improved consistency is also seen in the $w_0 - w_1$, $w_0 - w_2$, and $w_1 - w_2$ right-hand subpanels of Figures 17 and 18 for the $w_0w_1w_2$ CDM ($+A_L$) parametrizations, most prominently in the $w_0 - w_1$ subpanels.

From the numerical results for the $A_L = 1$ cases in Table 8, we see that at high- z the dynamical dark energy equation of state parameter $w(z \rightarrow \infty)$ is phantom-like at a significance of 1.52σ (w_0w_pp CDM), 2.17σ (w_0w_2 CDM), 2.20σ (w_0w_a CDM), and 2.88σ ($w_0w_1w_2$ CDM) for P18+lensing+non-CMB data. This support for dynamical dark energy over a cosmological constant can also be seen in Figures 5, 11, and 17; for the w_0w_a CDM parametrization see Ref. 19. We focus here on P18+lensing+non-CMB data, and so on the blue contours in the right-hand panels in these figures. In the $w_0 - w_2$ right-hand subpanel in Figure 5 for the w_0w_2 CDM parametrization we see that the Λ CDM model point at $w_0 = -1$ and $w_2 = 0$ lies outside the 2σ blue contour. The same is true for the $w_0 - w_p$, $w_0 - p$, and $w_p - p$ right-hand subpanels of Figure 11 for the w_0w_pp CDM parametrization, where the Λ CDM model corresponds to the point $w_0 = -1$ and $w_p = 0$, $w_0 = -1$ and $p = 0$, and $w_p = 0$ and $p = 0$, respectively, with the Λ CDM model points lying outside the 2σ blue contours in all three subpanels. In the right-hand $w_0 - w_1$, $w_0 - w_2$, and $w_1 - w_2$ subpanels of Figure 17 for the $w_0w_1w_2$ CDM parametrization, the Λ CDM model point $w_0 = -1$, $w_1 = 0$, and $w_2 = 0$ touches the 2σ blue contour in the $w_0 - w_1$ subpanel while lying outside the 2σ blue contours in the $w_0 - w_2$ and $w_1 - w_2$ subpanels.

From the numerical results for the varying A_L cases in Table 8, we see that at high- z the dynamical dark energy equation of state parameter $w(z \rightarrow \infty)$ is phantom-like at a significance of 1.05σ (w_0w_pp CDM $+A_L$), 1.35σ (w_0w_a CDM $+A_L$), 1.53σ (w_0w_2 CDM $+A_L$), and 1.76σ ($w_0w_1w_2$ CDM $+A_L$) for P18+lensing+non-CMB data, with $A > 1$ at a significance ranging from 1.83σ to 1.95σ depending on parametrization. This reduced support for dynamical dark energy over a cosmological constant (compared to the corresponding $A_L = 1$ case) can also be seen in Figures 6, 12, and 18; for the w_0w_a CDM $+A_L$ parametrization see Ref. 50. We again focus on P18+lensing+non-CMB data and so on the blue contours in the right-hand panels in these figures. In the $w_0 - w_2$ right-hand subpanel in Figure 6 for the w_0w_2 CDM $+A_L$ parametrization we see that the Λ CDM model point at $w_0 = -1$ and $w_2 = 0$ lies between the 1σ and 2σ blue contours. The same is true for the $w_0 - w_p$, $w_0 - p$, and $w_p - p$ right-hand subpanels of Figure 12 for the w_0w_pp CDM $+A_L$ parametrization, where the Λ CDM model corresponds to the

point $w_0 = -1$ and $w_p = 0$, $w_0 = -1$ and $p = 0$, and $w_p = 0$ and $p = 0$, respectively, with the Λ CDM model points lying between the 1σ and 2σ blue contours, but closer to the 1σ ones, in all three subpanels. In the right-hand $w_0 - w_1$, $w_0 - w_2$, and $w_1 - w_2$ subpanels of Figure 18 for the $w_0w_1w_2$ CDM+ A_L parametrization, the Λ CDM model point $w_0 = -1$, $w_1 = 0$, and $w_2 = 0$ touches the 2σ blue contours in the $w_0 - w_1$ and $w_0 - w_2$ subpanels while lying between the 1σ and 2σ blue contours in the $w_1 - w_2$ subpanel.

In summary, unlike in the flat Λ CDM (+ A_L) models, tables IV and VII in Ref. 58, in the dynamical dark energy parametrizations we consider, including the flat XCDM+ A_L parametrization, table XI of Ref. 58, and the flat w_0w_a CDM (+ A_L) parametrizations,^{19,50} and the flat w_0w_2 CDM (+ A_L), w_0w_pp CDM (+ A_L), and $w_0w_1w_2$ CDM (+ A_L) parametrizations, Tables 2–7, high- z P18 and P18+lensing data favor phantom-like dynamical dark energy, higher H_0 values, and smaller Ω_m values, all with larger error bars, while low- z non-CMB data favor quintessence-like dynamical dark energy, lower H_0 values, and larger Ω_m values, all with smaller error bars. Joint analysis of P18+lensing+non-CMB data breaks the parameter degeneracy and compromises by picking a slightly lower H_0 value and a slightly larger Ω_m value than are favored by non-CMB data but with much more restrictive error bars. Excluding the XCDM+ A_L case, in the two- and three-parameter $w(z)$ CDM cases the joint P18+lensing+non-CMB analysis results in a less, but still, phantom-like $w(z \rightarrow \infty) < -1$ when $A_L = 1$, which becomes even less, but still, phantom-like when A_L is allowed to vary and be simultaneously determined from these data. This evidence for phantom-like dark energy in these parametrizations is neither due to DESI BAO data (which we do not use), nor is it due to Pantheon+ or other SNIa data (see Refs. 19, 50 for analysis and discussion in the w_0w_a CDM case). Because all the parametrizations we study reduce to the XCDM parametrization at high z , all the parametrizations favor phantom-like dynamical dark energy at larger z . When $A_L = 1$ they favor phantom-like behavior at a significance of $\gtrsim 2\sigma$, while when A_L varies the significance drops to $\gtrsim 1\sigma$. This suggests that a significant part of the evidence for higher- z phantom-like behavior in these parametrizations is a consequence of the excess smoothing (relative to what is expected in the best-fit cosmological model) observed in some of the Planck CMB anisotropy multipoles.

5. Conclusion

Adding to the results of Refs. 19, 50, here we analyze three new $w(z)$ CDM (+ A_L) dynamical dark energy parametrizations. From where the Λ CDM model point lies relative to the P18+lensing+non-CMB data cosmological parameter constraint contours of the four $w(z)$ CDM (+ A_L) parametrizations, we find that dark energy dynamics is favored over a cosmological constant by $\gtrsim 2\sigma$ when $A_L = 1$, but only by $\gtrsim 1\sigma$ when A_L is allowed to vary (and is simultaneously determined from these data to be > 1 at $\sim 2\sigma$ significance). The non-CMB data compilation we use is the largest such compilation of independent, mutually-consistent non-CMB data.⁵⁸ It is

Is excess smoothing of Planck data partially responsible for DE dynamics in $w(z)$ CDM? 31

the dominant part of the P18+lensing+non-CMB compilation at low z when these data favor quintessence-like dark energy dynamics. At high z , when P18+lensing data are dominant, these data favor phantom-like dark energy dynamics, at significance ranging from 1.5σ to 2.9σ when $A_L = 1$ and at a reduced significance ranging from 1.1σ to 1.8σ when A_L is allowed to vary and be simultaneously determined from these data.

From ΔDIC values relative to the ΛCDM model, we find the $w(z)$ CDM parametrizations are *positively* favored over the ΛCDM model, for both the $A_L = 1$ (with ΔDIC values ranging from -2.45 to -3.98) and the varying A_L (with ΔDIC values ranging from -4.37 to -5.60) cases, with the varying A_L case *weakly to positively* favored over the $A_L = 1$ case (with relative ΔDIC values ranging from -1.62 to -2.15), because allowing A_L to vary results in better reconciliation of the P18 or P18+lensing data constraints and the non-CMB data constraints.

This evidence for dark energy dynamics in the $w(z)$ CDM parametrizations does not depend on the use of DESI data, which we have not used here, also see Refs. 19, 50. Nor does it depend on the use of Pantheon+ SNIa (or any SNIa data), see Ref. 19 for a detailed study of this in the w_0w_a CDM parametrization. The shifts toward quintessence-like behavior of the measured $w(z)$'s, in the $w(z)$ CDM ($+A_L$) parametrizations, when A_L is allowed to vary compared to the corresponding $A_L = 1$ case, suggest that this evidence for dark energy dynamics at least partially depends on the observed excess smoothing of some of the Planck CMB anisotropy multipoles, also see Ref. 50. In this context, it is interesting that from the new PR4 Planck data release,¹⁰⁰ in the flat $\Lambda\text{CDM}+A_L$ model, where A_L is allowed to vary, PR4 data including lensing data give $A_L = 1.037 \pm 0.37$, favoring $A_L > 1$ at 1σ , which is smaller than the 1.78σ significance for $A_L > 1$ that follows from the P18+lensing data result $A_L = 1.073 \pm 0.041$.

While our results are interesting, they are not based on a physically consistent dynamical dark energy model, e.g., ϕCDM ;^{101,102} they are based on $w(z)$ CDM parametrizations that reduce to different XCDM parametrizations at low and high z . Our results are also not that statistically significant. However, they highlight a number of interesting issues that deserve additional scrutiny.

Acknowledgments

C.-G.P. was supported by a National Research Foundation of Korea (NRF) grant funded by the Korea government (MSIT) No. RS-2023-00246367.

References

1. P. J. E. Peebles, *Astrophys. J.* **284** (1984) 439.
2. L. Perivolaropoulos and F. Skara, *New Astron. Rev.* **95** (2022) 101659, [arXiv:2105.05208 \[astro-ph.CO\]](#).
3. M. Moresco *et al.*, *Living Rev. Rel.* **25** (2022) 6, [arXiv:2201.07241 \[astro-ph.CO\]](#).
4. E. Abdalla *et al.*, *JHEAp* **34** (2022) 49, [arXiv:2203.06142 \[astro-ph.CO\]](#).

5. J.-P. Hu and F.-Y. Wang, *Universe* **9** (2023) 94, [arXiv:2302.05709 \[astro-ph.CO\]](#).
6. DESI Collaboration (A. G. Adame *et al.*) (4 2024) [arXiv:2404.03002 \[astro-ph.CO\]](#).
7. M. Chevallier and D. Polarski, *Int. J. Mod. Phys. D* **10** (2001) 213, [arXiv:gr-qc/0009008](#).
8. E. V. Linder, *Phys. Rev. Lett.* **90** (2003) 091301, [arXiv:astro-ph/0208512](#).
9. Y. Tada and T. Terada, *Phys. Rev. D* **109** (2024) L121305, [arXiv:2404.05722 \[astro-ph.CO\]](#).
10. W. Yin, *JHEP* **05** (2024) 327, [arXiv:2404.06444 \[hep-ph\]](#).
11. D. Wang (4 2024) [arXiv:2404.06796 \[astro-ph.CO\]](#).
12. O. Luongo and M. Muccino, *Astron. Astrophys.* **690** (2024) A40, [arXiv:2404.07070 \[astro-ph.CO\]](#).
13. M. Cortès and A. R. Liddle, *JCAP* **12** (2024) 007, [arXiv:2404.08056 \[astro-ph.CO\]](#).
14. E. O. Colgáin, M. G. Dainotti, S. Capozziello, S. Pourojaghi, M. M. Sheikh-Jabbari and D. Stojkovic (4 2024) [arXiv:2404.08633 \[astro-ph.CO\]](#).
15. D. Wang (4 2024) [arXiv:2404.13833 \[astro-ph.CO\]](#).
16. K. V. Berghaus, J. A. Kable and V. Miranda, *Phys. Rev. D* **110** (2024) 103524, [arXiv:2404.14341 \[astro-ph.CO\]](#).
17. H. Wang and Y.-S. Piao (4 2024) [arXiv:2404.18579 \[astro-ph.CO\]](#).
18. Y. Yang, X. Ren, Q. Wang, Z. Lu, D. Zhang, Y.-F. Cai and E. N. Saridakis, *Sci. Bull.* **69** (2024) 2698, [arXiv:2404.19437 \[astro-ph.CO\]](#).
19. C.-G. Park, J. de Cruz Pérez and B. Ratra, *Phys. Rev. D* **110** (2024) 123533, [arXiv:2405.00502 \[astro-ph.CO\]](#).
20. D. Shlivko and P. J. Steinhardt, *Phys. Lett. B* **855** (2024) 138826, [arXiv:2405.03933 \[astro-ph.CO\]](#).
21. Z. Huang *et al.*, *Phys. Rev. D* **110** (2024) 123512, [arXiv:2405.03983 \[astro-ph.CO\]](#).
22. DESI Collaboration (R. Calderon *et al.*), *JCAP* **10** (2024) 048, [arXiv:2405.04216 \[astro-ph.CO\]](#).
23. B. R. Dinda, *JCAP* **09** (2024) 062, [arXiv:2405.06618 \[astro-ph.CO\]](#).
24. D. Andriot, S. Parameswaran, D. Tsimpis, T. Wrase and I. Zavala, *JHEP* **08** (2024) 117, [arXiv:2405.09323 \[hep-th\]](#).
25. DESI Collaboration (K. Lodha *et al.*) (5 2024) [arXiv:2405.13588 \[astro-ph.CO\]](#).
26. S. Bhattacharya, G. Borghetto, A. Malhotra, S. Parameswaran, G. Tasinato and I. Zavala, *JCAP* **09** (2024) 073, [arXiv:2405.17396 \[astro-ph.CO\]](#).
27. O. F. Ramadan, J. Sakstein and D. Rubin, *Phys. Rev. D* **110** (2024) L041303, [arXiv:2405.18747 \[astro-ph.CO\]](#).
28. P. Mukherjee and A. A. Sen, *Phys. Rev. D* **110** (2024) 123502, [arXiv:2405.19178 \[astro-ph.CO\]](#).
29. N. Roy (6 2024) [arXiv:2406.00634 \[astro-ph.CO\]](#).
30. H. Wang, Z.-Y. Peng and Y.-S. Piao (6 2024) [arXiv:2406.03395 \[astro-ph.CO\]](#).
31. J. J. Heckman, O. F. Ramadan and J. Sakstein (6 2024) [arXiv:2406.04408 \[astro-ph.CO\]](#).
32. I. D. Gialamas, G. Hütsi, K. Kannike, A. Racioppi, M. Raidal, M. Vasar and H. Veermäe (6 2024) [arXiv:2406.07533 \[astro-ph.CO\]](#).
33. A. Notari, M. Redi and A. Tesi, *JCAP* **11** (2024) 025, [arXiv:2406.08459 \[astro-ph.CO\]](#).
34. G. Liu, Y. Wang and W. Zhao (7 2024) [arXiv:2407.04385 \[astro-ph.CO\]](#).
35. L. Orchard and V. H. Cárdenas, *Phys. Dark Univ.* **46** (2024) 101678,

Is excess smoothing of Planck data partially responsible for DE dynamics in $w(z)$ CDM? 33

- arXiv:2407.05579 [astro-ph.CO].
36. V. Patel, A. Chakraborty and L. Amendola (7 2024) arXiv:2407.06586 [astro-ph.CO].
 37. H. Wang, G. Ye and Y.-S. Piao (7 2024) arXiv:2407.11263 [astro-ph.CO].
 38. T.-N. Li, P.-J. Wu, G.-H. Du, S.-J. Jin, H.-L. Li, J.-F. Zhang and X. Zhang, *Astrophys. J.* **976** (2024) 1, arXiv:2407.14934 [astro-ph.CO].
 39. W. Giarè, M. Najafi, S. Pan, E. Di Valentino and J. T. Firouzjaee, *JCAP* **10** (2024) 035, arXiv:2407.16689 [astro-ph.CO].
 40. B. R. Dinda and R. Maartens (7 2024) arXiv:2407.17252 [astro-ph.CO].
 41. J.-Q. Jiang, W. Giarè, S. Gariazzo, M. G. Dainotti, E. Di Valentino, O. Mena, D. Pedrotti, S. S. da Costa and S. Vagnozzi (7 2024) arXiv:2407.18047 [astro-ph.CO].
 42. J.-Q. Jiang, D. Pedrotti, S. S. da Costa and S. Vagnozzi, *Phys. Rev. D* **110** (2024) 123519, arXiv:2408.02365 [astro-ph.CO].
 43. A. C. Alfano, O. Luongo and M. Muccino, *JCAP* **12** (2024) 055, arXiv:2408.02536 [astro-ph.CO].
 44. B. Ghosh and C. Bengaly, *Phys. Dark Univ.* **46** (2024) 101699, arXiv:2408.04432 [astro-ph.CO].
 45. S. Pourojaghi, M. Malekjani and Z. Davari (8 2024) arXiv:2408.10704 [astro-ph.CO].
 46. J. a. Rebouças, D. H. F. de Souza, K. Zhong, V. Miranda and R. Rosenfeld (8 2024) arXiv:2408.14628 [astro-ph.CO].
 47. W. J. Wolf, C. García-García, D. J. Bartlett and P. G. Ferreira, *Phys. Rev. D* **110** (2024) 083528, arXiv:2408.17318 [astro-ph.CO].
 48. S. Roy Choudhury and T. Okumura, *Astrophys. J. Lett.* **976** (2024) L11, arXiv:2409.13022 [astro-ph.CO].
 49. X. Lu, S. Gao and Y. Gong (9 2024) arXiv:2409.13399 [astro-ph.CO].
 50. C.-G. Park, J. de Cruz Perez and B. Ratra (10 2024) arXiv:2410.13627 [astro-ph.CO].
 51. T.-N. Li, Y.-H. Li, G.-H. Du, P.-J. Wu, L. Feng, J.-F. Zhang and X. Zhang (11 2024) arXiv:2411.08639 [astro-ph.CO].
 52. G. Payeur, E. McDonough and R. Brandenberger (11 2024) arXiv:2411.13637 [astro-ph.CO].
 53. M. Ishak *et al.* (11 2024) arXiv:2411.12026 [astro-ph.CO].
 54. S. Akthar and M. W. Hossain (11 2024) arXiv:2411.15892 [astro-ph.CO].
 55. Q. Gao, Z. Peng, S. Gao and Y. Gong (11 2024) arXiv:2411.16046 [astro-ph.CO].
 56. X. T. Tang, D. Brout, T. Karwal, C. Chang, V. Miranda and M. Vincenzi (12 2024) arXiv:2412.04430 [astro-ph.CO].
 57. M. Berbig (12 2024) arXiv:2412.07418 [astro-ph.CO].
 58. J. de Cruz Perez, C.-G. Park and B. Ratra, *Phys. Rev. D* **110** (2024) 023506, arXiv:2404.19194 [astro-ph.CO].
 59. Planck Collaboration (N. Aghanim *et al.*), *Astron. Astrophys.* **641** (2020) A6, arXiv:1807.06209 [astro-ph.CO], [Erratum: *Astron. Astrophys.* 652, C4 (2021)].
 60. J. Solà, A. Gómez-Valent and J. de Cruz Pérez, *Mod. Phys. Lett. A* **32** (2017) 1750054, arXiv:1610.08965 [astro-ph.CO].
 61. J. Ooba, B. Ratra and N. Sugiyama, *Astrophys. J.* **866** (2018) 68, arXiv:1712.08617 [astro-ph.CO].
 62. J. Ooba, B. Ratra and N. Sugiyama, *Astrophys. Space Sci.* **364** (2019) 176, arXiv:1802.05571 [astro-ph.CO].
 63. C.-G. Park and B. Ratra, *Astrophys. J.* **868** (2018) 83, arXiv:1807.07421 [astro-ph.CO].

64. J. Solà Peracaula, A. Gómez-Valent and J. de Cruz Pérez, *Phys. Dark Univ.* **25** (2019) 100311, [arXiv:1811.03505 \[astro-ph.CO\]](#).
65. C.-G. Park and B. Ratra, *Phys. Rev. D* **101** (2020) 083508, [arXiv:1908.08477 \[astro-ph.CO\]](#).
66. N. Khadka and B. Ratra, *Mon. Not. Roy. Astron. Soc.* **497** (2020) 263, [arXiv:2004.09979 \[astro-ph.CO\]](#).
67. S. Cao, J. Ryan and B. Ratra, *Mon. Not. Roy. Astron. Soc.* **497** (2020) 3191, [arXiv:2005.12617 \[astro-ph.CO\]](#).
68. N. Khadka and B. Ratra, *Mon. Not. Roy. Astron. Soc.* **499** (2020) 391, [arXiv:2007.13907 \[astro-ph.CO\]](#).
69. S. Cao, J. Ryan and B. Ratra, *Mon. Not. Roy. Astron. Soc.* **504** (2021) 300, [arXiv:2101.08817 \[astro-ph.CO\]](#).
70. S. Cao, N. Khadka and B. Ratra, *Mon. Not. Roy. Astron. Soc.* **510** (2022) 2928, [arXiv:2110.14840 \[astro-ph.CO\]](#).
71. F. Dong, C. Park, S. E. Hong, J. Kim, H. Seong Hwang, H. Park and S. Appleby, *Astrophys. J.* **953** (2023) 98, [arXiv:2305.00206 \[astro-ph.CO\]](#).
72. M. Van Raamsdonk and C. Waddell, *JCAP* **06** (2024) 047, [arXiv:2305.04946 \[astro-ph.CO\]](#).
73. M. Van Raamsdonk and C. Waddell (6 2024) [arXiv:2406.02688 \[hep-th\]](#).
74. R. I. Thompson, *Universe* **10** (2024) 356, [arXiv:2409.06792 \[gr-qc\]](#).
75. E. Calabrese, A. Slosar, A. Melchiorri, G. F. Smoot and O. Zahn, *Phys. Rev. D* **77** (2008) 123531, [arXiv:arXiv:0803.2309 \[astro-ph\]](#).
76. J. de Cruz Pérez, C.-G. Park and B. Ratra, *Phys. Rev. D* **107** (2023) 063522, [arXiv:2211.04268 \[astro-ph.CO\]](#).
77. Planck Collaboration (N. Aghanim *et al.*), *Astron. Astrophys.* **641** (2020) A1, [arXiv:1807.06205 \[astro-ph.CO\]](#).
78. D. Brout *et al.*, *Astrophys. J.* **938** (2022) 110, [arXiv:2202.04077 \[astro-ph.CO\]](#).
79. S. Cao and B. Ratra, *Phys. Rev. D* **107** (2023) 103521, [arXiv:2302.14203 \[astro-ph.CO\]](#).
80. A. Challinor and A. Lasenby, *Astrophys. J.* **513** (1999) 1, [arXiv:astro-ph/9804301](#).
81. A. Lewis, A. Challinor and A. Lasenby, *Astrophys. J.* **538** (2000) 473, [arXiv:astro-ph/9911177](#).
82. A. Lewis and S. Bridle, *Phys. Rev. D* **66** (2002) 103511, [arXiv:astro-ph/0205436](#).
83. A. Lewis (2019) [arXiv:1910.13970 \[astro-ph.IM\]](#).
84. J.-P. Dai, Y. Yang and J.-Q. Xia, *Astrophys. J.* **857** (2018) 9.
85. W. Fang, W. Hu and A. Lewis, *Phys. Rev. D* **78** (2008) 087303, [arXiv:0808.3125 \[astro-ph\]](#).
86. F. Lucchin and S. Matarrese, *Phys. Rev. D* **32** (1985) 1316.
87. B. Ratra, *Phys. Rev. D* **40** (1989) 3939.
88. B. Ratra, *Phys. Rev. D* **45** (1992) 1913.
89. S. Joudaki *et al.*, *Mon. Not. Roy. Astron. Soc.* **465** (2017) 2033, [arXiv:1601.05786 \[astro-ph.CO\]](#).
90. W. Handley and P. Lemos, *Phys. Rev. D* **100** (2019) 023512, [arXiv:1903.06682](#).
91. W. Handley and P. Lemos, *Phys. Rev. D* **100** (2019) 043504, [arXiv:1902.04029](#).
92. W. Handley, *Phys. Rev. D* **103** (2021) L041301, [arXiv:arXiv:1908.09139 \[astro-ph.CO\]](#).
93. G. Chen and B. Ratra, *Publ. Astron. Soc. Pac.* **123** (2011) 1127, [arXiv:1105.5206 \[astro-ph.CO\]](#), [arXiv:1105.5206](#).
94. J. R. Gott, III, M. S. Vogeley, S. Podariu and B. Ratra, *Astrophys. J.* **549** (2001) 1, [arXiv:astro-ph/0006103](#).

Is excess smoothing of Planck data partially responsible for DE dynamics in $w(z)$ CDM? 35

95. E. Calabrese, M. Archidiacono, A. Melchiorri and B. Ratra, *Phys. Rev. D* **86** (2012) 043520, [arXiv:arXiv:1205.6753](#) [[astro-ph.CO](#)].
96. W. L. Freedman, B. F. Madore, I. S. Jang, T. J. Hoyt, A. J. Lee and K. A. Owens (8 2024) [arXiv:2408.06153](#) [[astro-ph.CO](#)].
97. A. G. Riess *et al.*, *Astrophys. J. Lett.* **934** (2022) L7, [arXiv:2112.04510](#) [[astro-ph.CO](#)].
98. Y. Chen, S. Kumar, B. Ratra and T. Xu, *Astrophys. J. Lett.* **964** (2024) L4, [arXiv:2401.13187](#) [[astro-ph.CO](#)].
99. S. Barua and S. Desai (12 2024) [arXiv:2412.19240](#) [[astro-ph.CO](#)].
100. M. Tristram *et al.*, *Astron. Astrophys.* **682** (2024) A37, [arXiv:2309.10034](#) [[astro-ph.CO](#)].
101. P. J. E. Peebles and B. Ratra, *Astrophys. J. Lett.* **325** (1988) L17.
102. B. Ratra and P. J. E. Peebles, *Phys. Rev. D* **37** (1988) 3406.